

# **Mg-Al Layered Double Hydroxide Nano-Carrier for Controlled Release of anti-inflammatory Drug.**

*A Thesis Submitted in Partial Fulfillment of the  
Requirement for the Degree*

**MASTER OF TECHNOLOGY (RESEARCH)**

By

**SOUMINI MONDAL**

Roll No. 612CR3007

Under the guidance of

**Dr. Sudip Dasgupta**



**Department of Ceramic Engineering**

**National Institute of Technology, Rourkela**



**NATIONAL INSTITUTE OF TECHNOLOGY**

**Rourkela, INDIA**

---

## **CERTIFICATE**

This is to certify that the thesis entitled “Mg-Al Layered Double Hydroxide Nano-Carrier for Controlled Release of Anti-inflammatory Drug,” is being submitted by Miss. Soumini Mondal (612CR3007), for the degree of Master of Technology (Research) in Ceramic Engineering to the National Institute of Technology, Rourkela. This is a record of bonafide research work carried out by her under my supervision and guidance. Her thesis, in my opinion, is worthy of consideration for the award of the degree of Master of Technology (Research) in accordance with the regulations of the Institute.

The results embodied in this thesis have not been submitted to any other university or institute for the award of a Degree.

**Dr. Sudip Dasgupta**

Assistant Professor

Department of Ceramic Engineering

National Institute of Technology, Rourkela.

## **DECLARATION**

I declare that this thesis is my own work and has not been submitted in any form for another degree at any University or other Institution. Derived Information from the literature of published work of others has been acknowledged in the text, and a list of references are given.

Date: 05-01-2016

SOUMINI MONDAL

## TABLE OF CONTENTS

<b>ACKNOWLEDGEMENT</b> .....	i
<b>ABSTRACT</b> .....	ii
<b>LIST OF FIGURES</b> .....	iv
<b>LIST OF TABLES</b> .....	vi

### **CHAPTER 1 :- INTRODUCTION**

1.1 LAYERED DOUBLE HYDROXIDE:- .....	1
1.2 LDH- DRUG NANOHYBRID:- .....	3
1.3 SUMMARY:- .....	4
1.4 REFERENCES:- .....	5

### **CHAPTER 2 :- LITERATURE REVIEW**

2.1 LAYERED DOUBLE HYDROXIDE AS A NANOCARRIER: .....	7
2.2 STATEMENT OF THE PROBLEM:- .....	14
2.3 REFERENCES: .....	16

### **CHAPTER 3 :- MOTIVATION & OBJECTIVE OF WORK**

3.1 MOTIVATION OF WORK:- .....	19
3.2 OBJECTIVE OF WORK:- .....	21

### **CHAPTER 4 :- EXPERIMENTAL WORK:-**

4. EXPERIMENTAL PROCEDURE: - .....	22
4.1 MATERIAL:- .....	22
4.2 METHOD:- .....	22
4.3 CHARACTERIZATION OF SYNTHESIZED POWDERS .....	26

## **CHAPTER 5 :- RESULTS & DISCUSSION**

5.1 XRD ANALYSIS:- .....	34
5.2 PARTICLE-SIZE ANALYSIS:- .....	41
5.3 TEM ANALYSIS:- .....	43
5.4 FTIR ANALYSIS:- .....	46
5.5 THERMAL ANALYSIS:- .....	49
5.6 FESEM ANALYSIS:- .....	52
5.7 CHN ANALYSIS:- .....	54
5.8 IN-VITRO DRUG RELEASE:- .....	55
5.9 DISSOLUTION STUDY USING ATOMIC ABSORPTION SPECTROSCOPY: .....	60
5.10 HEMOCOMPATIBILITY ANALYSIS:-.....	62
5.11 MTT ASSAY ANALYSIS:- .....	65
5.12 DNA FRAGMENTATION ANALYSIS:- .....	68
5.13REFERENCES: .....	72

## **CHAPTER 6 :- CONCLUSION & SCOPE OF FUTURE WORK**

6.1 CONCLUSION: .....	74
6.2 SCOPE OF FUTURE WORK:.....	75

# **ACKNOWLEDGEMENT**

I owe my deepest gratitude to my supervisor Prof. Sudip Dasgupta, for his excellent guidance, encouragement and support during my work. I feel proud that I am one of his students, and I consider myself extremely lucky to get the opportunity to work under his guidance. I truly appreciate and value his professional knowledge, esteemed supervision and encouragement from the beginning to the end of this thesis. I express my sincere thanks to Prof. Swadesh Pratihara, & Prof B.B. Nayak, Head of Department of Ceramic Engineering, for providing me all the departmental facilities required for the completion of Project. I am thankful to Prof. Mukesh Gupta, Department of Biomedical and Biotechnology Engineering. And Also Prof S.K. Patra Department of Life Science, National Institute of Technology, Rourkela, for his support in the biological studies for my project work. I am also very thankful to all the member of my scrutiny committee – Prof. S.K.Behara, Prof. J. Bera, Prof. S.K.Pal, Prof. Mukesh Gupta, Department of Biomedical and Biotechnology Engineering. I would also like thank Dr. Biswanath Kundu, Central Glass & Ceramic Research Institute for his kind help with TEM & EDAX characterizations. I take this opportunity to thank the other faculty members and the supporting staff members of the department of Ceramic Engineering for their timely co-operation and support at various phases of experimental work. I would like to extend a special thanks to my dear Parents MOM, DAD and Sister (Srijani) for their support.

I would like to thank my dear friends Kanchan Maji, Dr. Moonmoon Deb, Rupita Ghosh, Pinky De, Rupali Singh, Satyananda Behara, Ashley Thomas, Vinod Paul, for their valuable suggestions and encouragement. I would also like to thank all research scholars of the department for their support and the friendly atmosphere in the laboratory.

## **ABSTRACT**

Layered double hydroxides (LDHs), have been known for many decades as a catalyst and ceramic precursors, traps for anionic pollutants, and additives for polymers. Recently, their successful synthesis on the nanometer scale opened up a whole new field for their application in nanomedicine. Here we report the efficacy of  $\text{Mg}_{1-x}\text{Al}_x (\text{NO}_3)_x (\text{OH})_2$  LDH nanoparticles as a carrier and for controlled release of one of the non-steroidal anti-inflammatory drugs (NSAID), sodium salicylate.  $\text{Mg}_{1-x}\text{Al}_x (\text{NO}_3)_x (\text{OH})_2 \cdot n\text{H}_2\text{O}$  nanoparticles were synthesized using co-precipitation method from an aqueous solution of  $\text{Mg}(\text{NO}_3)_2 \cdot 6\text{H}_2\text{O}$  and  $\text{Al}(\text{NO}_3)_3 \cdot 9\text{H}_2\text{O}$ . Salicylate was intercalated in the interlayer space of Mg-Al LDH after suspending nanoparticles in 0.0025(M)  $\text{HNO}_3$  and 0.75 (M)  $\text{NaNO}_3$  solution and using anion exchange method under  $\text{N}_2$  atmosphere. The shift in the basal planes like (003) and (006) to lower  $2\theta$  value in the XRD plot of intercalated sample confirmed the increase in basal spacing in LDH, which is because of intercalation of salicylate into the interlayer space of LDH. FTIR spectroscopy of SA-LDH nano hybrid revealed a red shift in the frequency band of carboxylate group in salicylate indicating an electrostatic interaction between cationic LDH sheet and anionic drug. Differential thermal analysis of LDH-SA nanohybrid indicated higher thermal stability of salicylate in the intercalated form into LDH as compared to its free state. DLS studies showed a particle size distribution between 30-60 nm for pristine LDH whereas salicylate intercalated LDH exhibited a particle size distribution between 40-80 nm which is ideal for its efficacy as a superior carrier for drugs and biomolecules. The cumulative release kinetic of salicylate from MgAl-LDH-SA hybrids in phosphate buffer saline (PBS) at pH 7.4 showed a sustained release of salicylate up to 72 h. The drug release kinetic closely resembled first order release kinetics through a combination of drug diffusion and dissolution of LDH under physiological conditions. The hemocompatibility tests performed on the samples showed that Mg Al LDH was compatible with human blood. Cytotoxicity of LDH-

SA nanohybrid was determined using MTT assay, subsequently the DNA fragmentation test on human kidney cells. The results suggest that SA intercalated into LDH was much less cytotoxic than the bare SA on kidney cells.

.

Keywords: Mg-Al LDH, Sodium Salicylate, Drug Delivery.



## **LIST OF FIGURES:**

FIGURE NO .	DESCRIPTION	PAGE NO .
FIGURE 1	Schematic representation of Layered Double Hydroxide.	1
FIGURE 2	Role of Layered Double Hydroxides as a functional material.	12
FIGURE 3	Schematic representation for different LDH applications.	19
FIGURE 4	(a) XRD pattern of synthesized Mg-Al LDH nanopowder.  (b) Comparative study of XRD pattern of Pristine LDH and Salicylate intercalated LDH nanopowder .	34  35
FIGURE 5	XRD Pattern of Pristine LDH and LDH -SA nanohybrid prepared using anion exchange method .	36
FIGURE 6	Schematic representation of salicylate intercalation into Mg Al LDH	37
FIGURE 7	(a) XRD pattern of Mg-Al LDH nanopowder at pH 8.  (b) Comparative study of XRD pattern of Pristine LDH and Salicylate intercalated LDH nanopowder .	38  39
FIGURE 8	(a) Particle size distribution of Pristine LDH.  (b) Particle size distribution of LDH-SA nanohybrid using coprecipitation method.  (c) Particle size distribution of LDH-SA nanohybrid prepared using anion exchange method	41  41  42
FIGURE 9	TEM micrographs of : -  (a) Pristine LDH (b) LDH - SA nanopowders prepared using co - precipitation (c) LDH -SA prepared using anion exchange	43

FIGURE 10	FTIR Spectroscopy of Pristine LDH, LDH-SA, Salicylic Acid powder.	46
FIGURE 11	(a) Thermogravimetric plot of LDH, SA, LDH-SA nanopowders (b) Differential thermal analysis (DTA) of LDH, SA and LDH-SA nanopowders.	49 50
FIGURE 12	FESEM analysis of (a) Mg-Al LDH nanopowder (b) Mg-Al LDH-SA nanohybrid.	52
FIGURE 13	FESEM analysis of (a) Heat – treated Mg-Al LDH nanopowders (b) Mg-Al LDH-SA reconstructed nanohybrid.	53
FIGURE 14	Release kinetics of SA from LDH-SA in PBS (pH-7.4 ) at 37 ° C.	55
FIGURE 15	Fit of first order release kinetic data to observed release rate.	55
FIGURE 16	Release kinetic fitted to zero order reaction kinetic.	57
FIGURE 17	Release kinetic fitted to Higuchi model.	57
FIGURE 18	Release kinetic fitted to Rigfus- Peppas model.	58
FIGURE 19	Release kinetic fitted to Korsmeyer- Peppas model.	58
FIGURE 20	Dissolution kinetic of Mg-Al LDH in PBS of pH 7.4	60
FIGURE 21	Samples prepared for the hemolysis test	63
FIGURE 22	Percentage hemolysis of free SA, LDH, and LDH –SA nanohybrid.	64
FIGURE 23	Reaction showing conversion of MTT to Formazan.	66

FIGURE 24	Cytotoxicity analyzes of Mg-Al LDH, SA & LDH –SA at 25 – 1.562 µg/mL on HEK 293 cells using the MTT assay.	66
FIGURE 25	Effect of MEM + FBS media on the HEK 293 cells	68
FIGURE 26	Effect of (a) Media (control) (b) LDH (c) SA (d) LDH-SA on the HEK 293 cells after 24 hrs of treatment	69
FIGURE 27	Effect of (a) Media (control) (b) LDH (c) SA (d) LDH-SA on the HEK 293 cells after 48 hrs of treatment	70
FIGURE 28	Agarose gel electrophoresis of DNA fragmentation analysis on HEK 293 cells (a) Lane 1: Control (b) Lane 2: LDH (c) Lane 3: SA (d) Lane 4: LDH-SA.	71

### **LIST OF TABLES:**

TABLE NO.	DESCRIPTION	PAGE NO
TABLE I	EDS analysis of LDH and LDH-SA nanopowders.	45
TABLE II	CHN analysis of LDH and LDH-SA nanopowders.	54
TABLE III	Drug release kinetic parameters derived from UV- visible spectrophotometer.	59
TABLE IV	Interpretation of diffusional release mechanisms from LDH- SA nano hybrid.	59
TABLE V	The OD values obtained after the hemocompatibility test for LDH, SA, and LDH-SA nanohybrid.	63
TABLE VI	Percentage Hemolysis for the three samples against the OD values	64

# CHAPTER 1: -

## **INTRODUCTION**

## 1.1 LAYERED DOUBLE HYDROXIDE:-

Numerous efforts have been made in recent times to develop novel drug carrier for transport, storage, and release of the drug at the targeted sites in the human body. Such nanocarriers exhibit numerous advantages over conventional forms of dosage that include enhanced bioavailability, greater efficacy and safety, controlled and prolonged release time, and unpredictable therapeutic response [1]. So far, a large number of materials have been employed as various drug delivery systems, such as biodegradable polymers, hydroxyapatite, xerogels, hydrogels [1], guar gum nanoparticles [2], fluoride hollow structures[3], superparamagnetic nanoparticles [4,5], functionalized mesoporous materials [6–8] etc. Layered double hydroxides (LDHs) [9] being one of the most efficient drug carrier amongst these, are widely used. LDHs are considered to be the new generation materials, comprising a two-dimensional layered structure similar to that of mineral brucite,  $\text{Mg}(\text{OH})_2$ [10].

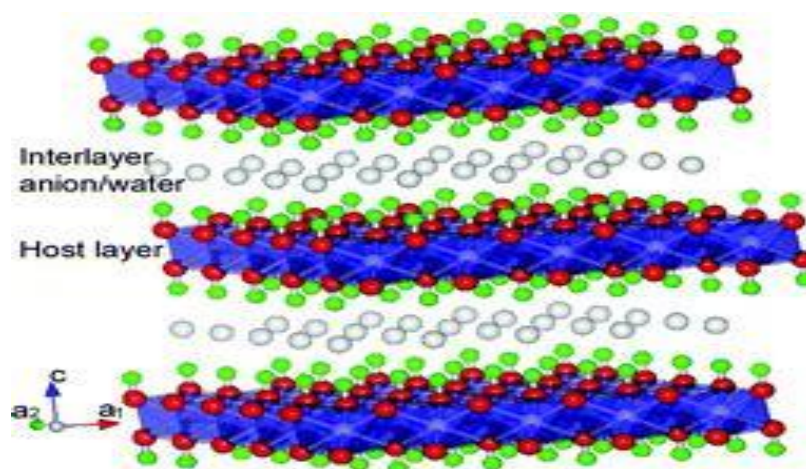


FIGURE 1: Schematic representation of Layered Double Hydroxide.

Layered Double Hydroxides (LDHs) are a special type of ceramic with hydrotalcite-like clay material. They have surface layers formed of positively charged brucite layers made up of mixed metal hydroxides of divalent and trivalent metals, with exchangeable intercalated negatively charged species in between the two surface layers. This negative charge

compensates for the positive charge of the brucite layer as shown in figure 1. Chemical composition of LDH is expressed as  $M(II)_{1-x} M(III)_x (OH)_2 (An^-)_{x/n} \times y H_2O$ , where  $M(II)$  is divalent metal cation,  $M(III)$  is trivalent metal cation. 'A' is an interlayer anionic species. And 'n' is the charge on the interlayer anion, 'x' and 'y' are fraction constants. The brucite type layer is of the structure with hydroxyl (OH) groups in hexagonal close packing, and each divalent metal cation was octahedrally coordinated to six OH<sup>-</sup> groups. These octahedra share edges to form the layers. Because all octahedrally coordinated cations occupied sites between oxygen layers, this structure is described as trioctahedral; each OH<sup>-</sup> group surrounded by three occupied octahedral positions. LDH have many physical and chemical properties that are surprisingly similar to those of clay mineral. These properties are their layered structure, wide chemical compositions (due to the variable isomorphous substitution of metallic cations), variable layer charge density, ion-exchange properties, reactive interlayer space and rheological and colloidal properties. But because of their anion-exchange properties, LDHs are also known as "anionic clays." The activated Mg Al-LDH film proved promising to be used as a precursor to synthesize monolithic catalyst for aldol condensation of acetone and other base-catalyzed reactions.[11] Structured LDHs were one new type of promising material due to their ability to capture organic and inorganic anions that could be used in water treatment. Layered double hydroxides (LDHs) had been known for many decades as catalyst and ceramic precursors, traps for anionic pollutants, catalysts and additives for polymers. But their successful synthesis on the nanometer scale a few years ago opened up a whole new field for their application in nanomedicine. LDHs are one of the ideal candidates for a wide range of agricultural applications. It is usually prepared under ordinary conditions of temperature, pressure, and so on, as a precipitate from solutions using environmentally benign methods. So it is easy to synthesize LDH with the desired anion(s) in the interlayer region for careful selection of the combination of metals and the organic compound. Among the many different nanoparticles that have been shown to facilitate gene and drug delivery,

LDH nanoparticles have attracted particular attention owing to their many desirable properties. Anionic drugs and functional biomolecules could easily be intercalated into the gallery space of LDH nanoparticles and also be released by deintercalation in the physiological system. Nanotechnology application to medicine has enabled the development of functionalized nanoparticles that, acts as carriers. They were loaded with drugs or genetic material that could be released with a controlled mechanism to specific sites of the organism [11]. Besides drug carrying capabilities, the functionalization of nanocarriers also facilitates their transport to primary target organs. Thus, bioavailability and efficiency of drug molecules is much more enhanced as being intercalated into the interlayer space of LDH as it can avoid enzymatic and environmental degradation during its circulation inside the body. Also, this category of nanocarrier is administrable via intravascular/pulmonary route and may be used for simultaneous targeted (chemo/gene) therapy and molecular imaging. Besides drug carrying capabilities, the functionalization of nanocarriers also facilitates their transport to primary target organs.

## 1.2 LDH- DRUG NANOHYBRID:-

LDH-drug nanohybrids have a positive zeta potential. Therefore, the nanohybrid particles can approach and adhere to the negatively charged cell membrane via electrostatic interaction. These nanohybrids can be internalized into the cell by phagocytosis (LDH agglomerates, particles larger than 500nm) and endocytosis (individual crystallite of smaller size, < 300nm). Endocytosis leads to quicker uptake of LDH nanoparticles. The cellular uptake can be enhanced by decreasing the particle size, adjusting the zeta potential and conjugating the ligands to enhance the receptor-mediated endocytosis process. Using LDH as drug delivery agent is advantageous. This is because of its easy preparation, particle size control, versatile composition, very good biocompatibility, pharmaceutical antacid behavior, very low cytotoxicity, controllable surface charge density, and easy attachment of targeting moiety.

Similar to intercalation process, de-intercalation can also occur by ion exchange method with the surrounding ions such as  $\text{Cl}^-$  and phosphates. A possible release pathway is the acidic dissolution of hydroxide layer due to the low pH in the intracellular environment. This is the only pathway for release of big anionic species.

### 1.3 SUMMARY:-

Anti-cancerous drug molecules such as methotrexate, 5-fluorouracil and anti-inflammatory drug molecules such as ibuprofen are negatively charged. Hence, those can be intercalated into the LDH molecule for its delivery into targeted location in the human body. As many of the biomolecules were negatively charged, they can also be intercalated into LDH including specific gene and DNA. Powdered LDHs have been described to be one of the most important green carriers or hosts for genes and drugs due to their excellent biocompatibility, bioresorbability and nontoxicity or low toxicity. MgAl-LDH finds application as an important component of drugs, or as nanocarriers for delivery of drug and genes into cells [13,14]



#### 1.4 REFERENCES:-

1. P.P. Yang, Z.W. Quan, C.X. Li, X.J. Kang, H.Z. Lian, J. Lin, Bioactive, luminescent and mesoporous europium-doped hydroxyapatite as a drug carrier, *Biomaterials* 29 (2008) 4341–4347.
2. R.S. Soumya, S. Ghosh, E.T. Abraham, Preparation and characterization of guar gum nanoparticles, *Int. J. Biol. Macromol.* 46 (2010) 267–269.
3. C.M. Zhang, C.X. Li, C. Peng, R.T. Chai, S.S. Huang, D.M. Yang, Z.Y. Cheng, J. Lin, Facile and controllable synthesis of monodisperse  $\text{CaF}_2$  and  $\text{CaF}_2\text{:Ce}^{3+}/\text{Tb}^{3+}$  hollow spheres as efficient luminescent materials and smart drug carriers, *Chem. Eur. J.* 16 (2010) 5672–5680.
4. S. Ghosh, D. Carty, S.P. Clarke, S.A. Corr, R. Tekoriute, Y.K. Gun'ko, D.F. Brougham, NMR studies into colloidal stability and magnetic order in fatty acid stabilized aqueous magnetic fluids, *Phys. Chem. Chem. Phys.* 12 (2010) 14009–14016.
5. J.K. Stolarczyk, S. Ghosh, D.F. Brougham, Controlled growth of nanoparticle clusters through competitive stabilizer desorption, *Angew. Chem. Int. Ed.* 48 (2009) 175–178.
6. S.L. Gai, P.P. Yang, C.X. Li, W.X. Wang, Y.L. Dai, N. Niu, J. Lin, Synthesis of magnetic, upconversion luminescent, and mesoporous core– shell structured nanocomposites as drug carriers, *Adv. Funct. Mater.* 20 (2010) 1166–1172.
7. S.S. Huang, Y. Fan, Z.Y. Cheng, D.Y. Kong, P.P. Yang, Z.W. Quan, C.M. Zhang, J. Lin, Magnetic mesoporous silica spheres for drug targeting and controlled release, *J. Phys. Chem. C* 113 (2009) 1775–1784.

8. P.P. Yang, Z.W. Quan, Z.Y. Hou, C.X. Li, X.J. Kang, Z.Y. Cheng, J. Lin, A magnetic, luminescent and mesoporous core-shell structured composite material as a drug carrier, *Biomaterials* 30 (2009) 4786–4795.
9. A.I. Khan, L.X. Lei, A.J. Norquist, D. O'Hare, Intercalation and controlled release of pharmaceutically active compounds from a layered double hydroxide, *Chem. Commun.* 234 (2001) 2–2343.
10. V. Rives, Characterisation of layered double hydroxides and their decomposition products, *Mater. Chem. Phys.* 75 (2002) 19–25.
11. Lv, Z.; Zhang, F.; Lei, X.D.; Yang, L.; Xu, S.L.; Duan, X. *In situ* growth of layered double hydroxide films on anodic aluminum oxide/aluminum and its catalytic feature in aldol condensation of acetone. *Chem. Eng. Sci.* **2008**, 63, 4055-4062.
12. . A Maria. Sabatinob, G.Adamoa, N. Grimaldib , C. Dispenza,c, and G. Ghersia. Polymeric Nanogels: Nanocarriers For Drug Delivery Application.,
13. S.-J Choi, J.-M Oh, J.-H. Choy, Human-related application and nanotoxicology of inorganic particles: Complementary aspects. *J. Mater. Chem.* **2008**, 18, 615-620.
14. Xu, Z.P.; Qing, H.Z.; Gao, Q.L.; Ai, B.Y. Inorganic nanoparticles as carriers for efficient cellular delivery. *Chem. Eng. Sci.* **2006**, 61, 1027-1040.

## CHAPTER 2: -

### **LITERATURE REVIEW**

## 2.1 LAYERED DOUBLE HYDROXIDE AS A NANOCARRIER:

Layered double hydroxides (LDHs) are well established as excellent anion exchange materials. The tremendous scope for fine tuning the intercalation and deintercalation kinetics of LDHs were originated because of its variable chemical composition, physical and structural properties. It employs different LDHs with differing charge densities and basicities. Because of the strong electrostatic interaction, multivalent anions within the interlayer space of LDH are particularly preferred. [1]

Intercalation of LDH with a variety of anions of pharmaceutical interest, such as salicylate, citrate, glutamate, and aspartate, was shown by Trontoet *al.*[2] Two different synthesis methods, a direct one (co-precipitation) and an indirect one (anion exchange of dodecyl sulfate samples) were used by authors. Variety of other molecules of biological interest such as ascorbic acid [3], biocatalysts [4], porphyrin [5], nucleotides [6], vitamins [7], amino acids and peptides [8,9] have also been intercalated into layered double hydroxides.

Intercalation of non-ionic pentoses (ribose and 2-deoxyribose) into the Mg-Al and Zn-Al layered double hydroxides at ambient temperature was shown by Aisawa et al.[10], using the calcination-rehydration reaction with precursors being calcined at 500°C. In another study intercalation of several amino acids into Mg-Al LDH was investigated by Hibino et al [11].

As a model for a drug delivery system intercalation of adenosine triphosphate (ATP) into Mg-Al LDH was studied by Tamura *et al* [12]. Being biocompatible systems [13], LDHs were used in pharmaceutical technologies[14,15] and medicine as drug supports or matrices. The drug release rate is governed by the pH once encapsulated. Several pharmaceutical applications as excipients, drug stabilizers, [16, 17] ingredients in sustained-release have been found using Mg-Al LDH. This hybrid was also used for the therapy of digestive disorders [18] and the preparation of aluminum magnesium salts of antipyretic, analgesic and anti-inflammatory drugs.

Khan et al. showed intercalation of a series of cardiovascular, anti-inflammatory and analgesic agents like diclofenac, gemfibrozil, ibuprofen, naproxen, 2-propylpentanoic acid, 4-biphenylacetic acid and tolfenamic acid into Li-Al-layered double hydroxide [19]. This drug-inorganic hybrid material acts as a novel tunable drug delivery system. Ambrosial *al.*[20] found that all chloride ions of hydrotalcite-like compounds exchanged by ibuprofen anions, which produced an intercalation compound with a drug loading of 50% w/w.

LDHs also acts as matrices for intercalation of non-steroidal anti-inflammatory drugs like Diclofenac [21]. Gordijo et al reported the immobilization of ibuprofen and copper-ibuprofen drugs on layered double hydroxides [22] Ion exchange, reconstruction, and coprecipitation reactions were used for the intercalation of ibuprofen into the LDH matrix. Immobilization of the drug and the copper-ibuprofen were performed by adsorption on the external LDH surfaces.

*In vivo* pharmacological study on the interaction between hydrotalcite and indomethacin was carried out by Del Arco *et al* [23]. They showed that intercalation of the drug simultaneously reduced the ulcerating damage of the drug. The intercalated compounds thus obtained with all anti-inflammatory drugs were hybrid systems, which, at room temperature, exhibited fluid and solid state properties. Hydrotalcite quickly dissolves in acidic *pH* thus releasing the drug in molecular form. Synthesis and characterization of nanoscale magnetic drug-inorganic composites by direct co-precipitation was carried out by Sun *et al* [24] and Zhang *et al.*[25]. They also reported captopril (Cpl) and 5-aminosalicylic acid (5-ASA) intercalation in Zn-Al LDH coated on MgFe<sub>2</sub>O<sub>4</sub> magnetic core particles.

The design and synthesis of *c-myc* antisense oligonucleotide (*As-myc*)-LDH hybrid by simple ion exchange method was performed by Kwak *et al* [26]. *As-myc* has a detectable function in cells, it represents a useful model system that helps to study the role of proto-oncogenes in cellular proliferation and differentiation. The negative charge on *As-myc* molecule allows easy intercalation into LDH by ion exchange that thermodynamically forms stable structure

due to enhanced electrostatic interaction. The transfer of *As-myc* into HL-60 cells through endocytosis, enhanced due to the charge neutralization. However, in the cells the other anions present in the cytosol would partially replace the interlayer oligonucleotides. The antisense oligonucleotide molecules was intercalated in the LDHs enter cells through endocytosis or phagocytosis process.

Leroux et al. reported the formation of Mg-Ga LDH-DNA nanohybrid using co-precipitation method. [27]. A parallel orientation of the DNA double helices in the interlamellar spaceways was indicated by the X-ray diffraction analysis. Inhibition of the crystal growth occurred due to the presence of adsorbed DNA macromolecules. The homogeneous populations of particles revealed that mean hydrodynamic diameters of macromolecules ranging from 90 to 150 nm, were compatible with cell penetration through endocytosis.

A novel method developed by Tyner *et al* [28], helped to deliver poorly water soluble drugs by intercalation into an LDH host. An alkaloid named camptothecin derived from the Chinese tree *camptotheca acuminata*. This alkaloid and its derivatives have unique ability to inhibit DNA topoisomerase, which traps the enzyme, thus inhibiting DNA replication and consequently killing the cancer cells. Successful intercalation of methotrexate (MTX), 5-fluorouracil (5-Fu) and folic acid (FA) into the interlayer space of Mg-Al-LDH was shown by Choy *et al.* [29-31]. Intercalation of these molecules into the hydroxide interlayer space was indicated by x-ray diffraction patterns and spectroscopic analyses, were found to be stabilized in the tilted longitudinal monolayer mode ( $46^\circ$  for MTX and  $50^\circ$  for folic acid) by electrostatic interaction. A drug-LDH system composed of MgAl-LDH and folate derivatives such as folic acid and methotrexate (MTX) were designed in the study of Gilman AG et al. [32]. They showed that folic acid finds application in therapy for different forms of cancers, prevention, and treatment of vitamin deficiencies [33]. The intercalation reaction took place without any deterioration of either LDH or drugs. Tumor cell suppression

was more efficient if MTX–LDH hybrid was used. So LDH could be used as an excellent inorganic carrier for an advanced biocompatible drug delivery system.

Qin et al. studied intercalation of folic acid using in-situ co-precipitation and anion exchange methods into Mg-Al-LDH.[34]. The stability of folic acid molecules between the hydroxide layers in LDH particles was demonstrated by XRD and also showed that it remained intact. The hybrid was constructed by both co-precipitation and ion exchange methods, with an interlayer spacing of 15.3 and 16.0 Å, respectively. UV-VIS method was used to calculate the drug loading in the hybrid system. It showed that nanohybrid prepared using co-precipitation route acquired heavier (19.32%) folic acid loading.

A biocompatible charge neutral Mg-Al LDH system had been built up by Wang et al. [35], through a calcination-restructure method, for the vehiculization of 5-FU. The interlayer arrangement of 5-FU depends on various patterns of aging treatment and different swelling solvents. The release studies showed a rapid 5-FU release from LDH during the first 40 min ( $\approx 65\%$  at pH4, and  $\approx 50\%$  at pH 7) that was followed by a slightly sustained one. The total amount of anti-cancerous drug released from the hybrid material was  $\approx 85\%$  at pH 4 and  $\approx 75\%$  at pH 7, after  $\approx 2.5$  hours. The different release mechanisms attributed to the differences in the release patterns between both pHs. At pH 7, the drug release mechanism was thought to be based on an ion-exchange process between 5-FU anions pillared in the lamella host and phosphate anions of the buffer solution. On the contrary, at pH 4 the LDH could start a dissolution process so that the faster 5-FU release occurred through ion-exchange and the removal of the inorganic host [36].

Manjusha Chakraborty, et al. [37] successfully synthesized Layered double hydroxide (LDH) – methotrexate (MTX) nanohybrid using ex-situ and in-situ processes. They showed that depending on the two synthesis routes used to synthesize LDH–MTX nanohybrid, its particle size as well as morphology could be varied at the nanoscale. LDH–MTX nanohybrid synthesized using in situ process exhibited lower aspect ratio as compared to ex-situ

synthesized LDH–MTX nanopowder. Nearly four times drug loading was exhibited by the ex-situ hydrothermal sample in comparison to the other two samples. The release behavior also corroborated the above observation and showed a controlled release profile of the drug delivery formulations. In their another paper [38], successful intercalation of MTX in the interlayer space of Zn-Al LDH was confirmed and suggested enhanced stability of MTX in the nano hybrid cationic framework.

Rossi et al. showed intercalation of ferulic acid into a hydrotalcite like LDH by a simple ion exchange process. [39]. The sunscreen properties of ferulic acid were potentially improved and protected from degradation and irradiation because of LDH. Thus, the intercalated compound could be formulated into a potentially useful silicone-based cream for sunscreen formulation. A new protection model designed by Perioli *et al* [40], where studies on the intercalation products of PABA into lamellar structures of Mg-Al and Zn-Al layered double hydroxides were reported. Feng et al. observed the interaction between the organic anion of 2-hydroxy-4-methoxy-benzophenone-5-sulfonic acid (HMBA) and Zn-Al-LDHs. [41]. HMBA-LDH intercalation system exhibited an enhanced photo- and thermal stability, it did not affect the UV absorption capacity.

Layered double hydroxides (LDH) have extensive applications as catalysts, catalyst precursors support, adsorbents, optical and electric functional materials, flame retardants and polymer stabilizers. Thus owing to the rich intercalation chemistry, LDH-based controlled release systems have recently gained particular attention. LDH powders and films widely explored as catalysts and adsorbed materials. The resulting activated structures obtained by calcination and rehydration, exhibit enhanced performances. Powdery LDHs are typically used as additives in flame retardants and concrete, and as a nanocarrier for drugs, gene molecules, biomedical products, and functional molecules. Ye Kuang et, al [42] discussed the preparation of novel LDH micro/nanostructures. They also developed the novel applications of these LDHs in many fields such as separation, catalyst, drug and gene delivery, and



electrode modifier for energy harvesting devices. Furthermore, the relationship between the novel structures and the enhanced properties of LDH micro/nanostructures, as well as understanding the specific structures prepared from confined nucleation and growth need to be explored. Our knowledge of controlled LDH nanostructures, resultant properties and applications would advance from these aspects.

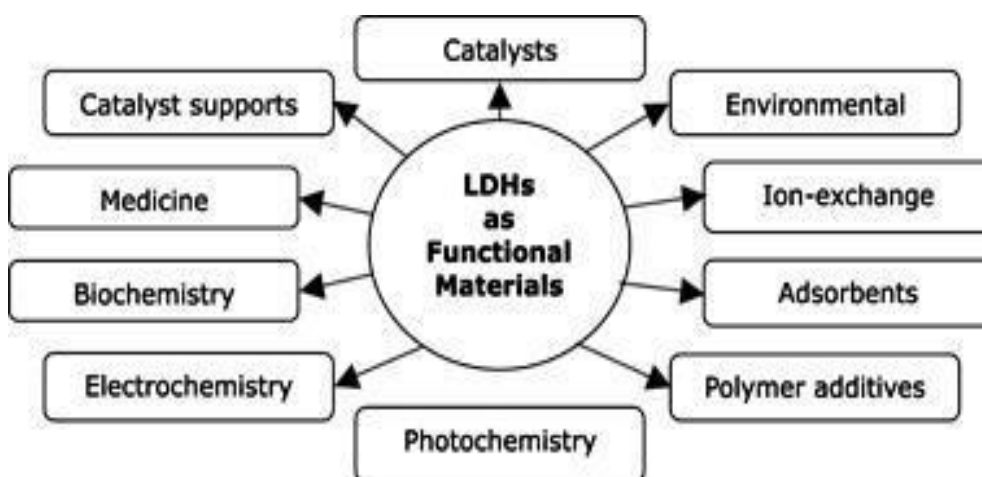


FIGURE 2: Role of Layered Double Hydroxides as a functional material

Hwang et al. reported the intercalation of vitamins A, E, and C into LDHs and zinc basic salts by coprecipitation method. [43, 44]. The hybrid was coated with a porous shell of silica to enhance the stability of intercalated vitamins and dispersion property of the hybrid nanoparticles. Bin Hussein et al. [45] reported dealing with LDHs for cosmetic applications and intercalated naphthol blue black into Mg Al-LDH, which made its formulation more easy and broad.

LDHs are one of the ideal candidates for a wide range of agricultural applications. Their framework could be decomposed into plant nutrients. Whereas their structure offered interesting features such as accommodation and controlled release of various active anionic agro-substances, high buffering capacity, high water retention ability, and acid neutralizing potential. Development of LDHs for agricultural purposes was not high and urgent, since

clays are naturally abundant and inexpensive, which is the important reasons for the retarded development of LDHs in agriculture. As serious contamination of soils and water arises from various anionic compounds, and development of the acidic property was found in cultivated soils, attempts of removal of anionic ions and pesticides by adsorption to LDHs have gained attention. Studies to develop the potential of LDHs as plant nutrients, pesticides, growth regulators, and active principle in animal feeds were carried out by Olanrewaju et al.[46]; Lakraimi et al. [47].

Synthesis of nitrate-LDH at ambient condition without any considerable contamination by carbonate was performed by Olanrewaju et al. [46], and found such LDHs as a potential slow-release fertilizer. Intercalation of plant growth regulator,  $\alpha$ -naphthalene acetate through coprecipitation was investigated by Bin Hussein et al. [45] to explore the protected storage and controlled release in natural environments. Pesticide formulations that mainly consisted of various organic solvents were given more attention. Intercalation of 2,4-dichlorophenoxy acetate, a broad leaf herbicide into ZnAl-LDH by ion exchange reaction was reported by Lakraimi et al. Therefore, the application of LDHs in agriculture could be more extensively expanded in near future as their acid neutralizing potential, and high anion adsorption capacity.

The sorption experiments carried out by Lucelena Patricio Cardoso et.al.[48] at different concentrations to obtain the isotherms, revealed that increasing anion concentration leads to the preferential intercalation of organic anions, which are arranged a bilayer in a position vertical to the LDH layers. The pH value of the organic anion solution did not exert any effect on the removal of these anions from the solution. All sorption isotherms had a very similar profile, and the number of removed anions at both pH values were close.

Reversible intercalation of phenoxy methyl penicillin into a layered double hydroxide was reported by Li et al. (2006) [49], and they showed that the resulting system exhibited effective anti-bacterial activity. In the pharmaceutical industry, LDHs are being used as

excipients and active principles. LDHs thus acting as laminar solids were revealed to be good excipients for anti-inflammatory drugs in formulations of controlled release as well as in solar protectors as reported by C Del Hoyo [50] et al. He also emphasized the importance in the synthesis of biosensors. LDHs can thus be considered as a group of promising materials in the development of new health applications.

Despite several fundamental studies on the mechanism by which LDH nanoparticles deliver their payload, only limited success has been found on efficient delivery of large biomolecules so far as reported by Katharina Ladewig et.al [51]. Most of the reports focus on intercalation and delivery of molecular drugs (anti-inflammatory drugs, anticancer drugs, etc.) and small nucleic acids (PCR fragments, antisense oligonucleotides, siRNA, etc.), which are quite promising for future bio-applications. Challenges remain involving dedication to the problem of well-dispersed LDH nanoplatelets to realize non-toxic, biocompatible and biodegradable LDH carries into practical applications for drug and gene delivery. Since targeting of drug/gene-carrying LDH materials is difficult because of the ionic nature of their surfaces, Oh et al. [52] and Xu et al. [53] presented two ways to circumvent the targeting problem. First approach was by functionalization of LDH nanoparticles through condensation of APS on LDH nanoparticle surface. Secondly by varying the morphology of the particles so that they target different intracellular compartments. Ion exchange using nitrate as the interlayer anion and co-precipitation after adding  $Mg^{2+}$  and  $Al^{3+}$  ions into a sodium salicylate solution were the two intercalation methods that were studied in this case.

## **2.2 STATEMENT OF THE PROBLEM:-**

Mg-Al-LDHs are widely used as a nanocarrier for delivery of non-steroidal anti-inflammatory drug in a controlled and sustained manner. Though the problem lies in the synthesis and processing of uniformly dispersed drug intercalated stable LDH suspension, in

the nano range of 50-100 nm, to maximize its bioavailability and retention capacity inside the cellular compartment.

Also, since these NSAIDs are very active in damaging kidney cells, the intercalation of NSAIDs into LDH may restrict the damaging capacity of NSAIDs to kidney cells, which has rarely being investigated. Here our objective is to study and optimize the synthesis parameter for obtaining uniform dispersed stable Mg-Al –LDH salicylate nanohybrid with an optimum size range in nanometre scale. We further investigate the effect of LDH-SA nanohybrid in restricting the damage of kidney cell while delivering the NSAID, through MTT Assay & DNA fragmentation test.

A detailed study on synthesis and characterization of Mg-Al-LDH-SA nanohybrid has been carried out for further understanding the controlled and sustained release behavior of SA, under physiological conditions.

## 2.3 REFERENCES:

1. M.Chakraborty, S.Dasgupta, S.Sengupta, J. Chakraborty and D.Basu, Layered Double Hydroxides Based Ceramic Nanocapsules as Reservoir and Carrier of Functional Anions, *Trans. Ind. Ceram. Soc.*, **69** (3) 153-163 (2010).
2. J. Tronto, E. L. Crepaldi, et al *Mol. Cryst. Liq. Cryst.*, **356**, 227-37 (2001).
3. J. H. Meng, H. Zhang, D. G. Evans and X. Duan, *Chin. Sci.Bull.*,**50**, 2575-81 (2005).
4. M. B. A. Rahman, M. Basri, M. Z. Hussein, M. N. H. Idris, R.N. Z. R. A. Rahman and A. B. Salleh, *Catal. Today*, **93-95**,405-10 (2004).
5. U. A. S. Barbosa, A. M. D. C. Ferreira and V. R. L. Constantino, *Eur. J. Inorg. Chem.*, **8**, 1577-84 (2005).
6. S. Aisawa, Y. Ohnuma, K. Hirose, S. Takahashi, H. Hirahara, E. Narita, *Appl. Clay Sci.*, **28**, 137-45 (2005).
7. S. H. Hwang, Y. S. Han and J. H. Choy, *Bull. Kor. Chem.Soc.*, **22**, 1019-22 (2001).
8. S. P. Newman, T. D. Cristina, P. V. Coveney and W. Jones, *Langmuir*, **18**, 2933-39 (2002).
9. P. Gerstel, R. C. Hoffmann, P. Lipowsky, L. P. H. Jeurgens, J. Bill and F. Aldinger, *Chem. Mater.*, **18**, 179-86 (2006).
10. S. Aisawa, H. Hirahara, K. Ishiyama, W. Ogasawara, Y. Umetsu and E. Narita, *J. Solid State Chem.*, **174**, 342-48(2003).
11. T. Hibino, *Chem. Mater.*, **16**, 5482-88 (2004).
12. H. Tamura, J. Chiba, M. Ito, T. Takeda and S. Kikkawa, *Solid State Ionics*, **172**, 607-609 (2004).
13. F. Cavani, F. Trifiro and A. Vaccari, *Catal. Today*, **11**, 173- 301 (1991).
14. U. Costantino and M. Nocchetti, pp. 3836-67 in *Layered Double Hydroxides. Present and Future*, Ed. V. Rives, NovaScience Publishers Inc, New York, USA (2001).
15. A. I. Khan, L. Lei, J. A. Norquist and D. O'Hare, *Chem.Comm.*,**22**, 2342-43 (2001).
16. M. Ueno and H. Kubota, US Patent no. 4,666,919 (1987).
17. N. Doi, A. Yonetani and T. Unno, Jpn. KokaiTokkyoKoho JP 01, 275-527 (1989).
18. Y. Hashimoto, H. Shiozawa, H. Kishimoto, and Y. Setoguchi, n PCT Int. Appl. JP 95-307512 (1997).
19. A.I. Khan, L. Lei, J. A. Norquist and D. O'Hare, *Chem.Comm.*,**22**, 2342-43 (2001).
20. V. Ambrogi, G. Fardella, e al *Int. J. Pharm.*, **220**, 23-32 (2001).

21. J. C. Dupin, H. Martinez, C. Guimon, E. Dumitriu and I. Fechete, *Appl. Clay Sci.*, **27**, 95-106 (2004).
22. C. R. Gordijo, C. A. S. Barbosa, A. M. D. C. Ferreira, V. R. L. Constantino and D. D. Silva, *J. Pharm. Sci.*, **94**, 1135-48 (2005).
23. M. del Arco, E. Cebadera, S. Gutiérrez, C. Martín, M. J. Montero, V. Rives, J. Rocha and M. A. Sevilla, *J. Pharm. Sci.*, **93**, 1649-58 (2004).
24. H. Sun, H. Zhang, D. G. Evans and X. Duan, *Chin. Sci. Bull.*, **50**, 752-57 (2005).
25. H. Zhang, K. Zou, H. Sun and X. Duan, *J. Solid State Chem.*, **178**, 3485-93 (2005).
26. S.-Y. Kwak, Y.-J. Jeong and J.-S. Park, *Solid State Ionics*, **151**, 229-34 (2002).
27. F. Leroux, M. B. Belkacem, G. Guyot, C. Taviot-Gueho, P. Leone, L. Cario, L. Desigaux and B. Pitard, *Org. Inorg. Hybrid Mater.*, **847**, 223-28 (2005).
28. K. M. Tyner, S. R. Schiffman and E. P. Giannelis, *J. Control. Release*, **95**, 501-14 (2004).
29. J.-H. Choy, J.-S. Jung, J.-M. Oh, M. Park, J. Jeong, Y.-K. Kang and O.-J. Han, *Biomaterials*, **25**, 3059-64(2004).
30. J.-M. Oh, M. Park, S.-T. Kim, J.-Y. Jung, Y.-G. Kang and J.-H. Choy, *J. Phys. Chem. Solids*, **67**, 1024-27 (2006).
31. S.-J. Choi, J.-M. Oh and J.-H. Choy, *J. Phys. Chem. Solids*, **69**, 1528-32 (2008).
32. Gilman AG, Goodman LS, Gilman A. The pharmacological basis of therapeutics. New York: Macmillan; 1980. p. 1272.
33. Lucock M. Folic acid: nutritional biochemistry, molecular biology, and role in disease processes. *Mol Genet Metab*2000;71:121–38.
34. L. Qin, S. Wang, R. Zhang, R. Zhu, X. Sun and S. Yao, *J. Phys. Chem. Solids*, **69**, 2779-84 (2008).
35. Z Wang, E Wang, L Gao, L Xu,. Synthesis and properties of Mg<sub>2</sub>Al layered double hydroxides containing 5-fluorouracil. *J. Solid State Chem.* **2005**, 178, 736-741.
36. José L. Arias, Novel Strategies to Improve the Anticancer Action of 5-Fluorouracil by Using Drug Delivery Systems, *Molecules* **2008**, 13, 2340-2369.
37. M.Chakraborty, S.Dasgupta & et al., Layered double hydroxide: Inorganic-organic conjugate nanocarrier for methotrexate, *Journal of Physics and Chemistry of Solids* 72 (2011) 779–783
38. M.Chakraborty et al., Methotrexate intercalated ZnAl-layered double hydroxide, *Journal of Solid State Chemistry* 184 (2011) 2439–2445.

39. C. Rossi, A. Schoubben, M. Ricci, L. Perioli, V. Ambrogi, L.Latterini, G. G. Aloisi and A. Rossi, *Int. J. Pharm.*, **295**, 47-55 (2005).
40. J.-H. Choy, S.-J. Choi, J.-M. Oh and T. Park, *Appl. Clay Sci.*, **36**, 122-32 (2007).
41. Y. J. Feng, et al *Polym. Degrad. Stab.*,**91**, 789-94 (2006).
42. .Ye Kuang et al, Morphologies, Preparations and Applications of Layered Double Hydroxide Micro-/Nanostructures, *Materials* 2010, 3, 5220-5235; doi:10.3390/ma3125220.
43. S.H Hwang, Y.S Han, J.H Choy, 2001. Intercalation of functional organic molecules with pharmaceutical, cosmeceutical and nutraceutical functions into layered double hydroxide and zinc basic salts. *Bull. Korean Chem. Soc.* 22, 1019-1022.
44. J.H Yang,, et al., 2003.Efficient transdermal penetration and improved stability of L-ascorbic acid encapsulated in an inorganic nanocapsule *Bull. Korean Chem.Soc.*24, 499–503.
45. Bin Hussein, et al., 2002. Controlled release of a plant growth regulator, alpha-naphthalene acetic from the lamella of Zn–Al-layered double hydroxide nanocomposite. *J. Control. Release* 82, 417–427.
46. J Olanrewaju, B.L Newalkar, C Mancino, S Komarneni, 2000. Simplified synthesis of nitrate form of layered double hydroxide.*Mater. Lett.* 45, 307–310.
47. M.Lakraimi, A Legrouri, A Barroug, De Roy, A., Besse, J.P., 2000. Preparation of a new stable hybrid material by chloride-2,4-dichloro phenoxy acetate ion exchange into the zinc–aluminum–chloride layered double hydroxide. *J. Mater. Chem.*10, 1007–1011.
48. Lucelena et al., Study of acids herbicides removal by calcined Mg—Al—CO<sub>3</sub>—LDH, *Journal of Physics and Chemistry of Solids* 67 (2006) 987–993.
49. Li, W.Z., J Lu, et al., 2006. Phenoxy methyl penicillin-intercalated hydrotalcite as a bacteria inhibitor. *J. ChemTechnol. Biotechnol.* 81 (1), 89–93.
50. C. Del Hoyo, Layered double hydroxides and human health: An overview, *Applied Clay Science* 36 (2007) 103 –121.
51. K. Ladewig et al., Layered Double Hydroxide Nanoparticles in Gene and Drug Delivery, *Expert Opin. Drug Deliv*(2009) 6(9):907 922.
52. J-M Oh, et al. Inorganic metal hydroxide nanoparticles for targeted cellular uptake through clathrin-mediated endocytosis. *Chem An Asian J* 2009;4(1):67-73.
53. Xu ZP, et al. Subcellular compartment targeting of layered double hydroxide nanoparticles. *J Control Release* 2008;130(1):86-94.

## CHAPTER 3:-

### **MOTIVATION & OBJECTIVE** **OF WORK**



### 3.1 MOTIVATION OF WORK:-

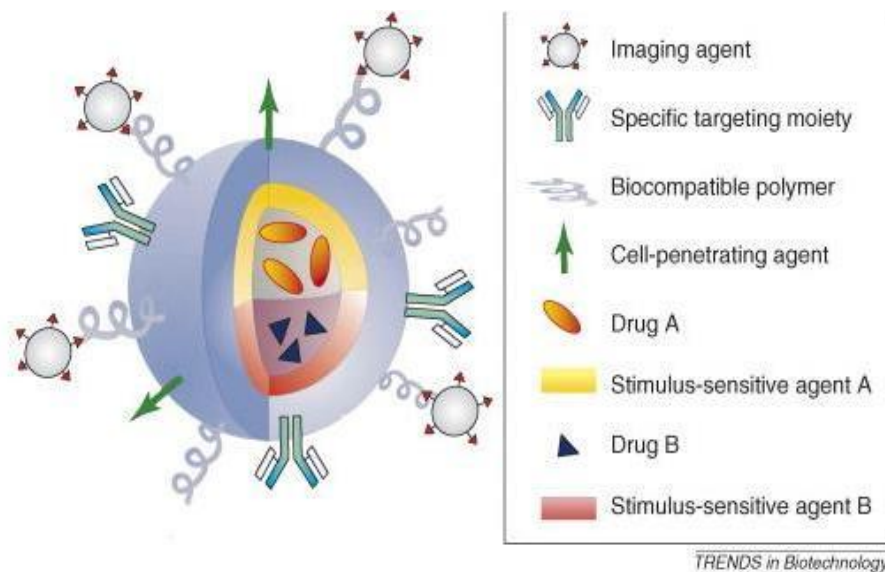


FIGURE 3: Schematic representation for different LDH applications

The factors behind the motivation for using LDH as a nanocarrier for drug delivery are discussed below:

➤ BIOCOMPATIBILITY:

The term refers to the ability of the material to perform with an appropriate host response in a specific situation. The ambiguity of the term reflects the ongoing development of insights into how the biomaterials interact with the human body and eventually how those interactions determine the clinical success of a medical device. In this context, Mg Al LDH is highly biocompatible.

➤ BIORESORBABLE :

The term refers to those the materials that can be broken down by the body.

That do not require any mechanical removals, such as sutures or the chlorhexidine chip. Mg al LDH nanoparticles are highly bioresorbable under physiological condition.

➤ CONTROLLED RELEASE:

The term refers to the presentation or delivery of compounds in response to stimuli or time. This could be for purposes in several areas including agriculture, cosmetics and personal care, pharmaceuticals, and food science. Most commonly here it refers to the time dependent release in oral dose formulations. Drugs in intercalated form inside the Mg Al LDH shows controlled and sustained release behaviour under physiological condition.

➤ HYDROPHILIC:

It refers to materials having an affinity for water; readily absorbing or dissolving in or be wetted by water. Hydrophilic molecules typically have polar groups enabling them to absorb readily or dissolve in water as well as in other polar solvents. Because of hydrophobicity, Mg Al LDH can easily escape the reticuloendothelial system (RES) of human body and avoid phagocytosis by macrophages.

➤ EASY SURFACE FUNCTIONALIZATION:

It introduces chemical functional groups to a surface. This way, materials with functional groups on their surfaces can be designed from substrates with standard bulk material properties. Prominent examples were found in the biomaterial research. Mg Al LDH can be easily surface functionalized for attributing multifunctional properties to it.

➤ EASY ENDOCYTOSIS:

The process by which a living cell takes up molecules bound to its surface. It involves cellular ingestion by which the plasma membrane folds inward to bring substances into the cell. Being positively charged Mg-Al LDH can easily be attracted into negatively charged interior compartment of cells through endocytosis.



### 3.2 OBJECTIVE OF WORK:

- Synthesis of LDH with positively charged layers having two kinds of metallic cations - divalent, e.g., Mg and trivalent, e.g., Al, of a general formula  $[M^{2+}_{1-x}M^{3+}_x(OH)_2]^{x+}(A^{n-})_{x/n} \cdot mH_2O$ , ( $x$  is equal to the molar ratio of  $M^{2+}/(M^{2+} + M^{3+})$  and  $A^{n-}$  is an anion) by co-precipitation under nitrogen atmosphere.
- Incorporation of anionic anti-inflammatory drug by anion exchange route.
- Characterization of LDH- drug nanohybrid using XRD, FTIR, dynamic light scattering technique, transmission electron microscopy.
- Estimation of drug loading using C, H, N or thermogravimetric (TGA) Analysis.
- Study on the drug release behavior of the LDH- drug nanohybrid under physiological pH in vitro.
- Study on cytotoxicity of Mg-Al LDH –SA nanohybrid on human embryonic kidney cells.

## CHAPTER 4:-

### **EXPERIMENTAL WORK:**

#### 4. **EXPERIMENTAL PROCEDURE:-**

##### 4.1 **MATERIAL:-**

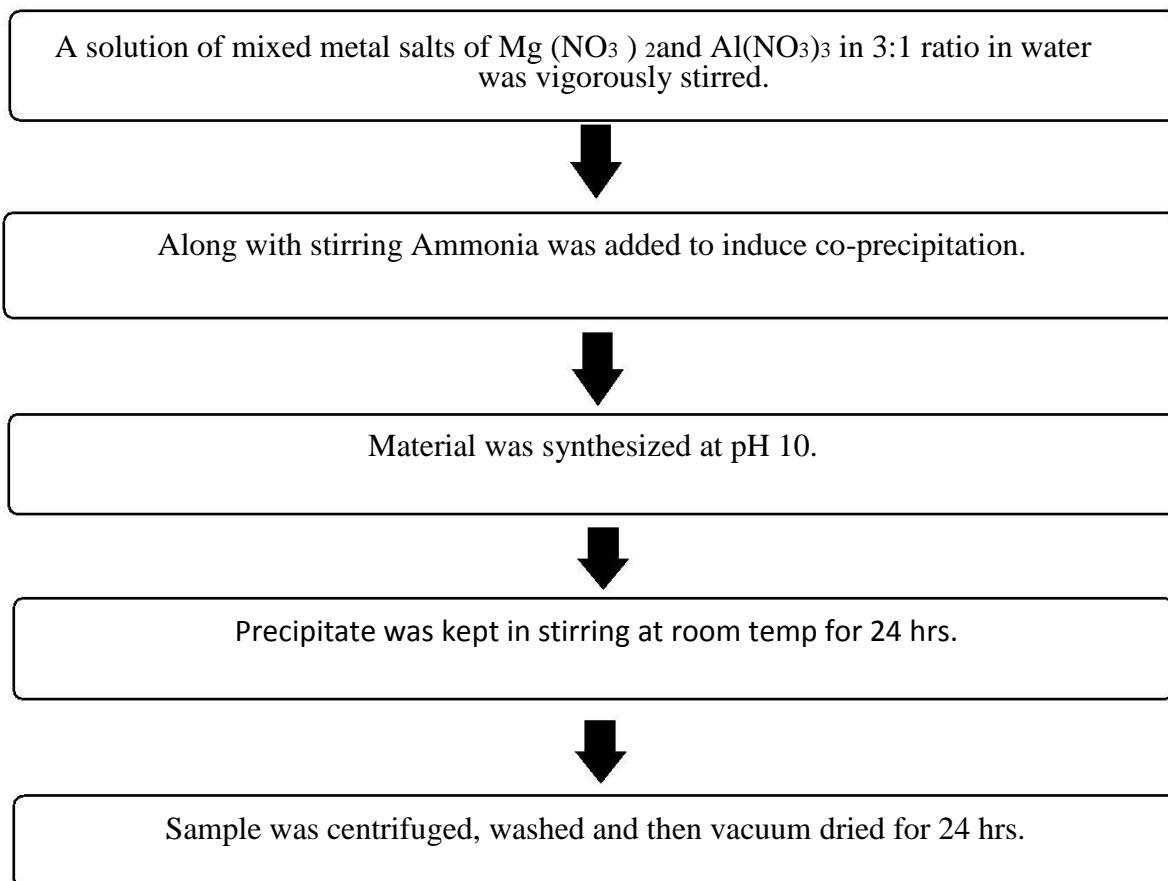
Magnesium nitrate hexahydrate [  $\text{Mg} (\text{NO}_3)_2 \cdot 6\text{H}_2\text{O}$ ], aluminum nitrate nonahydrate [ $\text{Al} (\text{NO}_3)_3 \cdot 9\text{H}_2\text{O}$ ], ammonium hydroxide [ $\text{NH}_4 \text{OH}$ ] were purchased from Sigma-Aldrich, USA. Sodium salicylate [NaOSal] was synthesized from salicylic acid [HOSal] (Merck, India) and sodium hydroxide [NaOH] (Merck, India). Deionized and decarbonated ultra-pure water (Millipore, specific resistivity  $18 \text{ M}\Omega$ ) was used in all preparations and the chemicals utilized in this study were used as received without further purification.

##### 4.2 **METHOD:-**

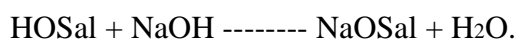
###### 4.2. 1 **SYNTHESIS OF Mg -Al LDH nanoparticle :-**

0.495 (M)  $\text{Mg} (\text{NO}_3)_2 \cdot 6\text{H}_2\text{O}$  (19.1262 g) and 0.165 (M)  $\text{Al} (\text{NO}_3)_3 \cdot 9\text{H}_2\text{O}$  (9.321 g) were dissolved in 150 ml of water to synthesize Mg-Al LDH with Mg: AL in ratio of 3:1. To maintain the pH of the mixed precursor solution at pH 10, ammonia was used, along with magnetic stirring. The stirring was continued for further 24 hours. The appearance of a white gelatinous precipitate indicated the formation of Mg-Al-LDH. The precipitate was collected by centrifugation and repeatedly washed by redispersing it in water followed by centrifugation (at 3000 rpm for 5mins) to remove excess nitrate anions. The washed LDH precipitate was then vacuum dried for 24 hrs to get Mg AL-LDH nanopowder. With a target amount of 3 grams of pristine LDH to be produced, 5 grams of  $\text{Mg}(\text{NO}_3)_2 \cdot 6\text{H}_2\text{O}$  and 0.6 grams of  $\text{Al}(\text{NO}_3)_3 \cdot 9 \text{H}_2\text{O}$  were taken . After the product obtained it was measured and found that amount of pristine LDH produced was 2 grams , which was calculated to be around 68 % of the theoretical yield.

#### Preparation of Mg Al Layered Double Hydroxide Nanoparticle:



#### 4.2.2 Synthesis of Sodium Salicylate from Salicylic Acid:-



One mole of Salicylic Acid reacts with one mole of Sodium Hydroxide in an aqueous medium to form a mole of sodium salicylate and a mole of water. The molar mass of NaOH is approximately 0.290 times that of salicylic acid (SA); thus 10 grams of SA would be reacted with 2.90 grams of NaOH.. It is important to use 1:1 molar ratio so that there would be no excess NaOH or SA in the final product. NaOH was dissolved in as little distilled water

as required to solubilize, whereas SA was dissolved in another beaker in a little amount of ethanol as required to solubilize it completely. The two solutions were mixed, subsequently heated at a temperature of 65 to 80° C and vigorously stirred on a stirrer until the solution thickened and became pale yellow. Finally, the crystals precipitated out and eventually became completely dry and thus Sodium Salicylate was obtained.

#### 4.2.3.1 Synthesis of Mg Al -Salicylate LDH hybrid nanoparticle using co - precipitation method : -

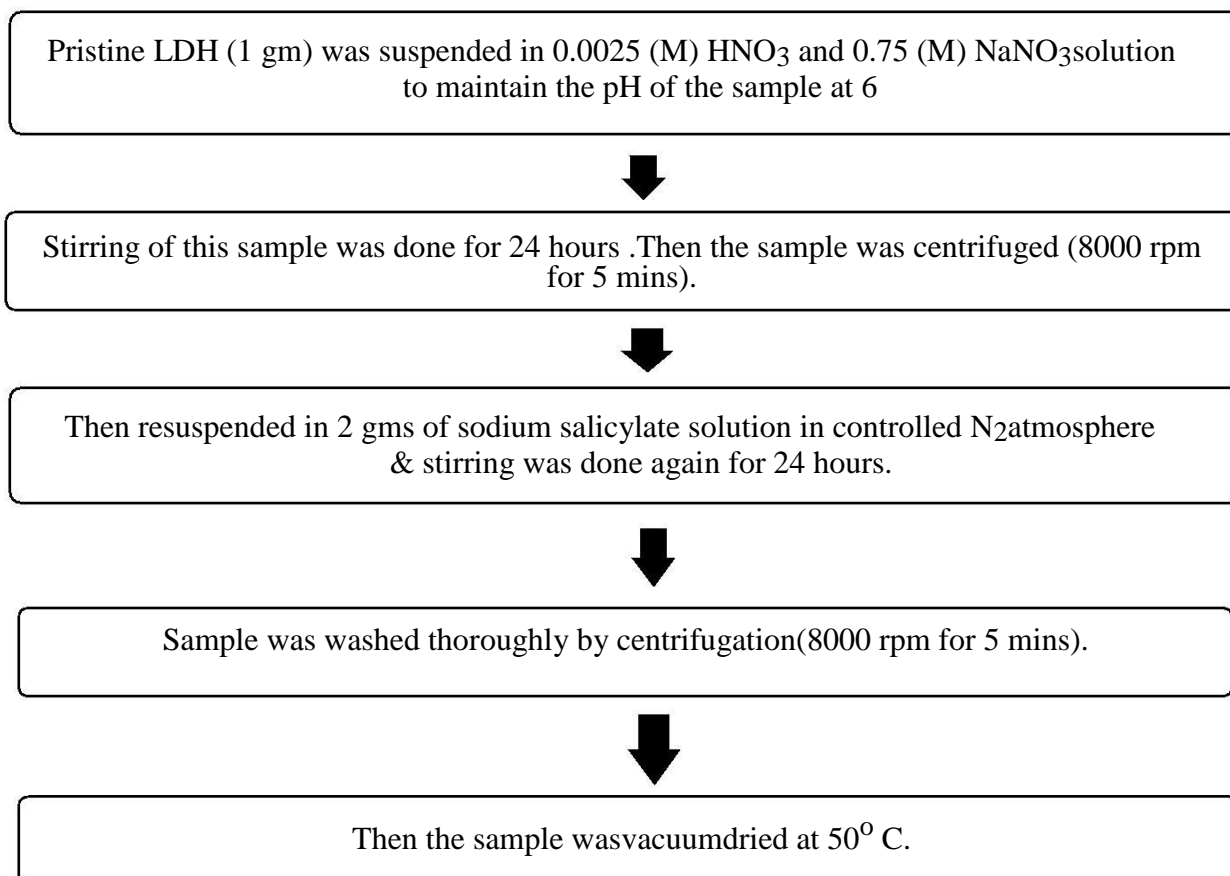
Intercalation of sodium salicylate into its interlayer space was also performed using the co - precipitation method . 0 .495 (M) Mg (NO<sub>3</sub>)<sub>2</sub>·6H<sub>2</sub>O (19.1262 g) and 0.165 (M) Al (NO<sub>3</sub>)<sub>2</sub>·9H<sub>2</sub>O (9.321 g) with Mg: Al in ratio of 3:1, were dissolved in 150 ml of water followed by addition of 1 gm of sodium salicylate under nitrogen atmosphere with constant stirring. To maintain the pH of the mixed precursor solution at pH 10, ammonia was used, along with magnetic stirring. The stirring was continued for further 24 hours in nitrogen atmosphere. The appearance of a white gelatinous precipitate indicated the formation of Mg-Al-LDH- SA hybrids. The sample was then centrifuged , washed with distilled water thrice to remove nitrate and excess salicylate and then vacuum dried.

#### 4.2.3.2 Synthesis of Mg Al -Salicylate LDH hybrid nanoparticle using anion exchange method : -

Subsequently after the preparation of the Mg - Al LDH particle and sodium Salicylate, it was now time for the intercalation of the sodium salicylate drug into the pristine LDH to obtain the Mg- Al LDH - salicylate nanohybrid. Two gm of salicylate was dissolved in 50 ml water of pH 7.5 (pH was raised by the addition of 25% NH<sub>4</sub>OH) and the solution was added to 100 ml aqueous suspension in 0.0025(M) HNO<sub>3</sub> and 0.75 (M) NaNO<sub>3</sub> containing 1 g of LDH. The pH of the LDH- Salicylate mixture was raised to 8.5 by dropwise addition of 0.01 M NaOH. The reaction mixture was agitated for 72



hours in a nitrogen atmosphere. The product, MgAl-LDH– Salicylate, was centrifuged, washed with deionized water and then dried in a vacuum oven at 50 °C.



#### 4.2.4 Preparation of PBS buffer solution:-

An Erlenmeyer flask filled with 800 ml of dd H<sub>2</sub>O was kept on a magnetic stirrer maintaining its speed uniformly. 0.8 g of NaCl, 0.2 g KCl, 1.44 g of Na<sub>2</sub>HPO<sub>4</sub> and 0.25 g of KH<sub>2</sub>PO<sub>4</sub> were added to the flask, and the solutes were allowed to dissolve for 3 to 5 minutes along with stirring. Before adjusting the pH of the solution, it was necessary to be ensured that there were no remaining undissolved salts in the solution. After stirring vigorously for 5 minutes, the speed of the stirrer was then slowed down. 1 M HCl was added dropwise to the solution using a pipette and mixed thoroughly in the solution. The pH of the

solution was measured with a calibrated pH meter. The pH of the solution was thus maintained at 7.4

#### 4.2.5 Preparation of samples for UV- Spectrophotometer Analysis:-

20 mg of MgAl LDH–Salicylate formulation was dispersed in 2 mL of PBS of pH 7.4 in 8 different eppendorfs, marked and kept at a constant stirring. After a definite time interval, one Eppendorf was taken at a time and centrifuged (at 3000 rpm for 5mins). The solvent was then collected in a tube, filtered through 0.2 µm filter paper and the filtrate was kept for analysis, using a UV-visible spectrophotometer.

### 4.3 Characterization of synthesized powders

#### 4.3.1 X-Ray Diffraction Method:-

X-ray diffraction relies on the dual wave/particle nature of X-rays to obtain information about the structure of crystalline materials. A primary use of the technique is the identification and characterization of compounds based on their diffraction pattern. Bragg's Law described the diffraction of X-rays by crystal,  $n\lambda = 2d \sin \theta$ , where  $\lambda$  = wavelength of x-ray,  $n$  = order of diffraction.]. The directions of possible diffractions depend on the size and shape of the unit cell of the material. Powder X-ray diffraction (XRD) patterns for MgAl LDH and MgAl LDH –Salicylate powders obtained with X'Pert High Score diffractometer (Rigaku, Japan) using  $\text{CuK}\alpha$  ( $\lambda$ - 1.5418° Å) radiation at 40 mA, 40 kV. A step size of 0.005° was used in the scan range 1-80° (2 $\theta$ ). The instrument model used here is X-Pert, PANalytical, PW 3040/00, Netherlands.

#### 4.3.2 Zetasizer –Particle Size Analysis:-

The particle size analyzer measures the size of the particle in a sample. It measures particle size in the size range of 1nm- 3µm. Dynamic light scattering at 90 degrees is used to measure

the particle size of the sample. It thus helps in the particle size determination of nanoparticles, surfactants, micelles, and colloids. The instrument model used here is MicrotracZetatrac, PA (USA).

#### 4.3.3 Transmission Electron Microscopy (TEM)

In this Transmission Electron microscope, an electron beam from an electron gun is transmitted through an ultra-thin section of the microscopic object and the image is magnified by the electromagnetic fields. It is used to observe finer details of internal structures of microscopic objects like bacteria and other cells. Particle size and morphology of LDH and LDH-SA nanohybrid powders were examined using a transmission electron microscope (TEM) (Tecnai G<sup>2</sup> 30ST FEI, Netherland) operated at an acceleration voltage of 120 KV.

#### 4.3.4 Fourier Transform Infra Red Spectroscopy (FTIR)

FT-IR stands for Fourier Transform Infrared, the preferred method of infrared spectroscopy. FTIR was used to characterize the chemical functional groups present in materials, based on the characteristics of vibrational and rotational energies of different molecular bonds. Fourier transform infrared (FTIR) spectra of the prepared powders were recorded at room temperature. KBr (Brooker,  $\geq 99\%$ ) pellet method (sample: KBr = 1:100) on a F Varian 3600 (USA) spectrometer in the  $400\text{--}4000\text{ cm}^{-1}$  range with an average of 10 scans were used. The instrument model used here is Perkin Elmer, USA/ RX-I FTIR.

#### 4.3.5 Differential Scanning Calorimetry (DSC) and Thermogravimetry (TG)

##### Analysis

The Differential Scanning Calorimetry (DSC) is a thermoanalytical technique in which the difference in the amount of heat required to increase the temperature of a sample relative to a reference material measured as a function of temperature. The working temperature can reach up to  $1500^{\circ}\text{C}$  in a controlled atmosphere. On the other hand, thermogravimetry (TG) determines the change in weight in relation to temperature. The DSC-TG instrument helps in

the determination of phase transition temperature, the heat of crystallization, weight loss in materials on heating, specific heat measurement, and study of reaction kinetics. The thermogravimetric (TG), and differential scanning calorimetry (DSC), of LDH and LDH-SA nanopowders were studied on 50 mg of powder samples using a TG/DSC analyser (Netzsch, Germany, STA449C/4/MFC/G.). The measurements were recorded from 50°C to 1000°C at 10°C/min heating rate in air.

#### 4.3.6 Field Emission Scanning Electron Microscopy (FESEM)

The FESEM stands for Field Emission Scanning Electron Microscope and facilitates ultra-high resolution microstructural characterization and analysis of ceramic and metallic samples. It combines advanced optics (including a two-mode final lens), SE/BSE (Secondary Electrons /Back-scattered Electrons) in-lens detection and beam decleration. Since being equipped with EDAX, it helps in composition mapping and elemental analysis. SEM images of the prepared sample were recorded with beam landing energy down to 50 V, and with a resolution of 1.4 nm @ 1 kV without beam deceleration. The instrument model used for the experiment is Nova Nano SEM/ FEI.

#### 4.3.7 CHN Analyzer:-

A CHN analyzer helps us to analyze the Carbon, Hydrogen, Nitrogen, Oxygen content of an unknown organic compound. This helps in identification of the product in terms of its molecular formula. The compound of interest combusted in a furnace at a high temperature under oxygen stream. During the combustion process mostly the oxides of the concerned elements were formed in the form of gases. They are then separated and directed to a detector consisting of inert gases like helium or argon as a carrier for quantitative analysis. Thus, measurement of carbon, hydrogen, and nitrogen contents of the sample are obtained with fair accuracy. The instrument model used here is Elemental Analysen Systeme, Germany / Vario EL.

#### 4.3.8 Atomic Absorption Spectroscopy:-

Atomic Absorption Spectroscopy determines the presence of metal in liquid samples in as low as ppm level. Metals absorb ultraviolet light in their elemental form when excited by heat. This instrument searches for a particular metal by focusing a beam of UV light at a specific wavelength range (190-900 nm) through a flame into a detector. The sample of interest was aspirated into the flame. The instrument then measures the intensity converting it into absorbance value. Samples tested and measured against calibrated curves constructed by running standards of various concentrations. Here 0.02 mg of Mg- Al LDH nanopowder was taken per ml of PBS buffer solution in small eppendorfs. The eppendorfs are marked and kept at constant stirring. Readings were taken after picking up of one eppendorf at a time, centrifuging it at 3000 rpm for 5 minutes, and then gently the solvent is collected in another eppendorf. The same procedure was followed with all the other test eppendorfs. The instrument model used here is AAS Shimadzu 24, Japan.

#### 4.3.9 UV-Visible Spectrometer:-

The process of identification and quantification of chemical species by measuring the absorption of monochromatic electromagnetic radiation having a wavelength in the UV-VIS range ( 200-900 nm) is referred to as UV- Visible spectroscopy. Routinely being used in analytical chemistry, for the quantitative determination of different analytes, such as transition metal ions, biological macromolecules, and highly conjugated organic compounds. The instrument model used here is Lambda 35, Perkin Elmer, USA.

20 mg of MgAlLDH–Salicylate formulation was dispersed in 2 mL of PBS of pH 7.4 in 8 different eppendorfs, marked and kept at a constant stirring. After definite time interval, one eppendorf was taken at a time and centrifuged (at 3000 rpm for 5 mins). The solution was

then collected in a tube, filtered through 0.2 µm filter paper and the filtrate was kept for analysis using a UV-visible spectrophotometer.

#### 4.3.10 HEMOCOMPATIBILITY Analysis:-

Hemocompatibility tests were done for the samples as per the American Society for Testing and Materials (ASTM) standard protocol. It figures out the extent of hemolysis, i.e. the rupture or destruction of red blood cells, in the presence of the three samples. Here for the tests to perform fresh goat blood was collected in the presence of TriSodiumCitrate (TSC). The hemocompatibility test were performed on 3 different samples, such as pristine Mg-Al – LDH (Mg: Al=2:1), Mg-Al –LDH intercalated with salicylic acid, and pure salicylic acid (SA). 0.05 g of each of these samples were taken in the tubes followed by the addition of 9.5 ml of saline in each of the tubes. For positive control, 0.5 ml of diluted blood was mixed with 0.1 N HCl and subsequently diluted to 10 ml. As HCl has the ability to rupture the Red Blood Cells it can act as a positive control. For the negative control 0.5 ml of blood was diluted to 10 ml with the Saline solution. The centrifuge tubes were then incubated at 37°C for 60 minutes (1 hour) in Oswald BOD incubator (IRIC-10). After being incubated, they were centrifuged at 4000 rpm for 10 minutes. Finally, the Optical Density (OD) of all the samples were measured at 545 nm using a UV-visible Spectrophotometer. The percentage (%) hemolysis was calculated as per the following formula:-

$$\% \text{ Hemolysis} = \frac{OD_{\text{test}} - OD_{\text{Negative}}}{OD_{\text{positive}} - OD_{\text{Negative}}} \times 100$$

If the % hemolysis is <5 then the material is considered as highly hemocompatible, a value <10 indicates hemocompatible whereas a value > 20 indicates non-hemocompatible.

#### 4.3.11 MTT ASSAY Analysis:-

The term MTT assay refers to a colorimetric assay used for assessing cell metabolic activity. This assay was performed to measure the cell viability, assessed through, 'color-change' phenomenon from yellow colored tetrazolium salt, MTT {3-(4,5-diamethyl thiazol-2-yl)-2,5-diphenyltetrazolium bromide} to purple colored formazan. These cell viability and cytotoxicity assays used for drug screening and cytotoxicity tests of chemicals were performed on HEK293 cells commonly known as the Human Embryonic kidney cells. The HEK 293 cells were taken, and their culturing was done in an MEM (Minimum Essential Media) mixed with 10 % FBS (Foetal Bovine Serum) media. This mixture provides the complete nutrition for the cells to flourish. Stored cells were thus retrieved and seeded in 96 well plates containing the media and kept for growth in a CO<sub>2</sub> incubator (Heracell 150i, Thermospecific). A controlled atmosphere of 37°C and 5 % CO<sub>2</sub> was maintained. To obtain a dose response effect of the drug, the drug of interest was diluted to 5 different concentration. In the growth media in parallel, the cells were thus treated with the controlled media to assess its effect on cells. Cells were treated with three samples such as pristine LDH, LDH-SA and free SA at various concentration and the cells were incubated upto 48 hours at 37°C. The samples without any LDH or SA addition was treated as positive control. To detect the cell viability, the MTT working solution was prepared by diluting the stock solution (stock 5 mg /mlPBS, pH-7.2) in growth media without FBS to the final concentration of 0.8 mg/ml. 100 µl of MTT working solution was added to each well and again incubated for 4 hours in a CO<sub>2</sub> incubator. After incubation, the media was carefully removed without disturbing the formazan precipitate and dissolved in 100 µl of 100 % DMSO. Hence again incubated in the dark for 15 minutes and the colorimetric estimation was performed on a microplate reader at 570 nm.

#### 4.3.12 DNA FRAGMENTATION Analysis:-

This test clearly indicates the effect of the ceramic Mg-Al LDH nanomaterial, bare salicylic drug and the Mg-Al LDH-SA nanohybrid on the HEK 293 cells. The protocol used for this experiment provided a qualitative method for assessing cell death by detecting the DNA fragments using agarose gel electrophoresis. One of the classic features of cell death is the cleavage of the genomic DNA into oligonucleosomal fragments represented by multiples of 180 – 200 base pairs. Characterization of this event could be aided by visualizing these fragments. The reagents used for this experiment were the agarose gel, Ethidium Bromide, TAE [Tris base, Acetic acid, EDTA], TES lysis buffer.

The cells were taken and centrifuged at 2000 rpm in an Eppendorf using a table top centrifuge for 5 mins at 4°C, and the supernatants were removed. 20µl of TES lysis buffer added and the cell pellets were mixed with it. After the addition of 10 µl of RNase cocktail, the cells were incubated for 120 minutes at 37° C. Consecutively 10µl of Proteinase K was added, and the cells were incubated at 50°C for overnight. The cells are then taken out of incubation and loaded into dry wells of a 1-1.5 % agarose gel in TAE containing 0.5µg/ml ethidium bromide. The gel was run at a low voltage that helps to improve the resolution of the DNA fragments. DNA ladders were finally visualized by a UV light source and documented by photography.

#### 4.4 STATISTICAL STUDIES:

All data are expressed as mean  $\pm$  standard deviation. The datas were compared using students t – test and differences were considered significant, when  $p < 0.05$ . A p – value more than 0.05 ( $p > 0.05$ ) was taken as an indication of no significant difference.



## CHAPTER 5: -

### **RESULTS & DISCUSSION**

## 5.1 XRD ANALYSIS:-

Phase evaluation of hydrotalcite-like LDH material was performed using XRD. The pristine MgAl-LDH (3:1) precursor was prepared using co-precipitation of the component hydroxides at constant pH with carbonate and exchangeable nitrate anions in the gallery space. Here

Figure 4 (a) shows the powder XRD patterns of pristine Mg-Al LDH.

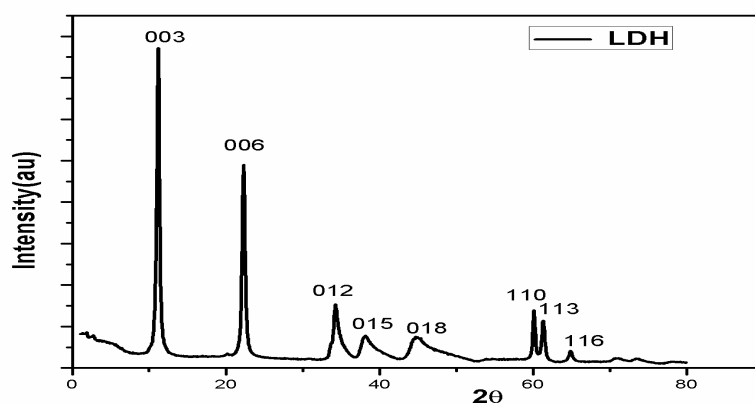


FIGURE 4 (a): XRD pattern of synthesized Mg-Al LDH nanopowder

The presence of both sharp and diffuse non-basal reflections in the XRD plot were taken as an indication of a partially disordered structure, resulted due to irregular stacking superposition of the regular unit layers. The pattern for MgAl - LDH was characteristic of the LDH structure with reasonably well crystallized hydrotalcite -like phase exhibiting rather sharp and symmetric 00l reflections. The basal spacing for (003), ( $d_{003}$ ) was estimated to be 7.94 Å in pristine

MgAl - LDH . The powder XRD diffractogram of the LDH sample showed the structure of hydrotalcite displaying the characteristic reflection . Firstly with sharp and intense basal 00l reflections of 003 and 006 planes in the low angle region ( $2\theta < 25^\circ$ ). Secondly broad 0kl reflections of 012, 015, and 018 planes in the middle angle region

( $2\theta = 30^\circ$ - $50^\circ$ ), and (iii) sharp  $hk0$  and  $hkl$  reflections of 110, 113, and 116 planes, in the high angle region ( $2\theta = 55^\circ$ - $65^\circ$ ). The short-range order in the brucite-like sheet of hydrotalcite were reported by Brindley and Kikkawa [1]. The formation of a supercell with a 2:1 Mg/Al ratio (corresponding to the maximum observed substitution of Mg by Al, thus  $x = 0.33$ ) was also observed in some minerals by Taylor [2]. It was thus verified on the basis of geometric considerations. At higher Al content ( $x > 0.33$ ), Al octahedra would become adjacent, thus leading to nucleation of  $Al(OH)_3$ . With a Mg/Al ratio higher than 4 ( $x < 0.20$ ), the location of the Mg ion favours the formation of brucite. In this case 3:1 Mg/Al ( $x=0.25$ ) was taken as a precursor to synthesize Mg-Al layered double hydroxides.

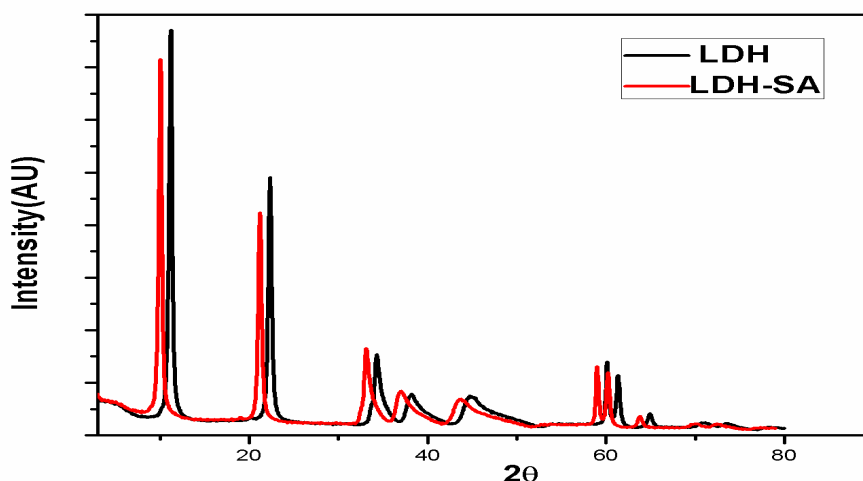


FIGURE 4( b): Compar ative study of XRD pattern of Pristine LDH and Salicylate intercalated LDH nanopowder .

Here figure 4(b) shows the comparative XRD pattern of pristine LDH and LDH-SA nanohybrid synthesized using coprecipitation method, where SA remained intercalated into interlayers of LDH. The intercalation of salicylate into the MgAl-LDH matrix was evidenced by the shift of (003), (006) planes to higher  $d$ -values (Fig 1b). The gallery space for MgAl-LDH-salicylate hybrid material was found to be 8.90 Å, which was higher than the longitudinal molecular length of 6.25 Å for salicylate molecule. The basal spacing ( $d_{003}$ )

increased from 7.94 Å in MgAl-LDH to that 8.90 Å in MgAl-LDH–salicylate hybrid because of intercalation of SA into the interlayer space of LDH.

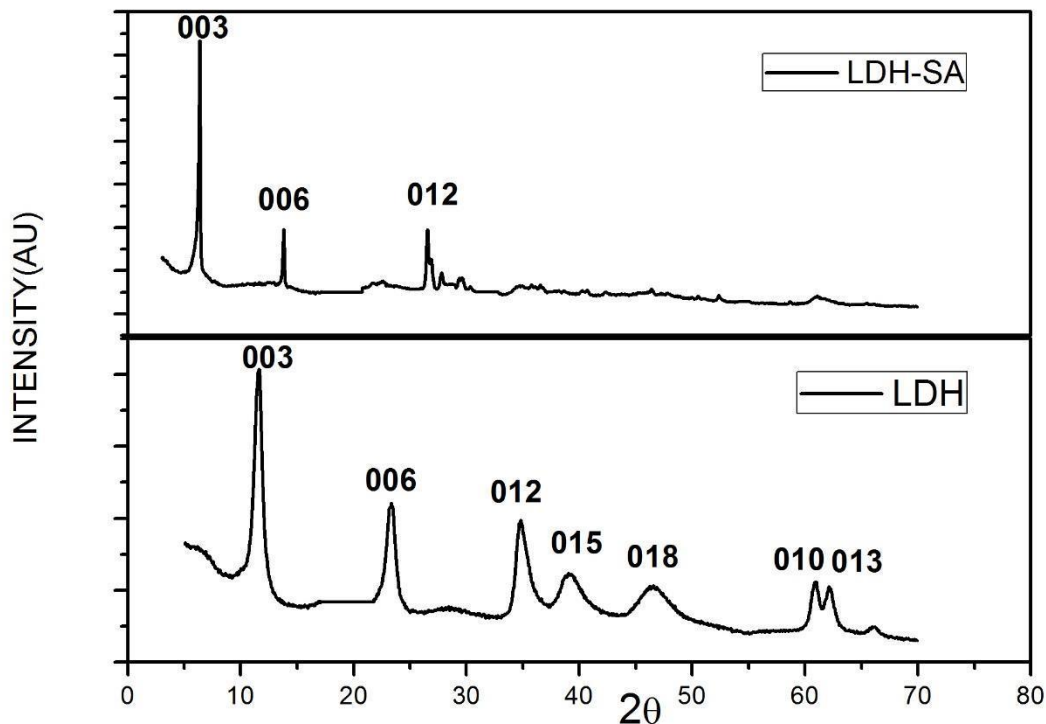


FIGURE 5: XRD Pattern of Pristine LDH and LDH -SA nanohybrid prepared using anion exchange method.

Figure 5 shows the comparative XRD pattern of pristine LDH and LDH –SA nanohybrid prepared using anion exchange method . The  $d(003)$  value for LDH was increased from 7.94Å to 19.25Å in LDH -SA nanohybrid because of intercalation of long chain salicylate interlayer space and thereby expanding  $d(003)$  lattice phase. The carbonated LDH was transformed into nitrate containing Mg -Al LDH on exposure to the suspension, containing 0.0025 (M)  $\text{HNO}_3$  and 0.75 (M)  $\text{NaNO}_3$  solution . The mild acidic condition decomposes the carbonate inside the LDH, keeping the LDH structure intact, and instead of

non-exchangeable carbonate/nitrate ions occupied the interlayer space of Mg-Al LDH.

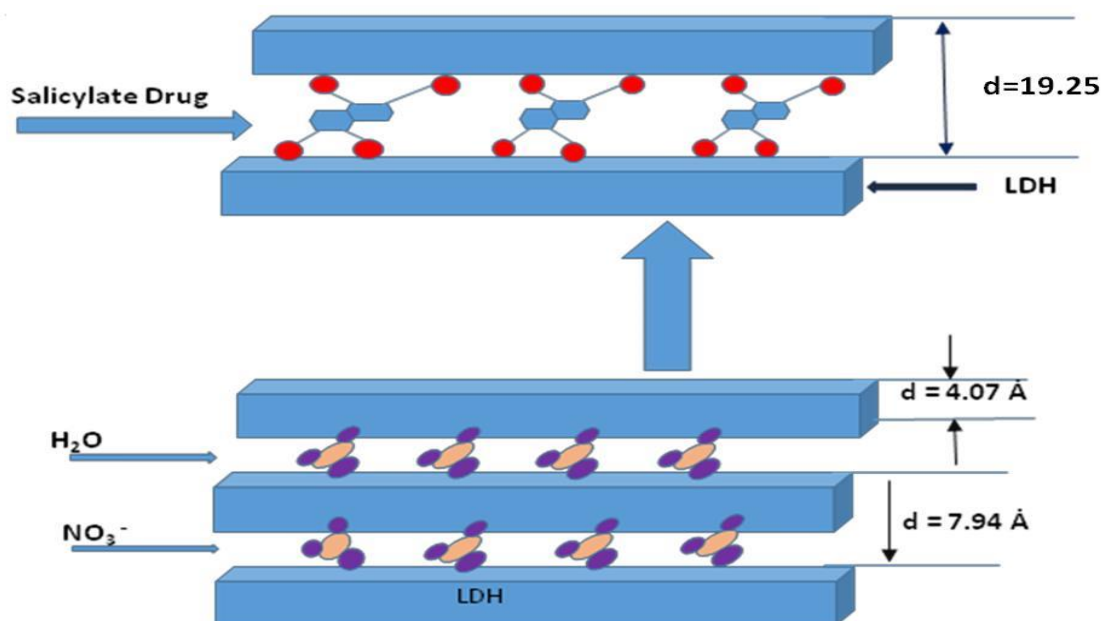


FIGURE 6 : Schematic representation of salicylate intercalation into Mg-Al LDH

A schematic presentation of the intercalation of Salicylate into the LDH interlayers is shown in Fig. 6. Salicylate ion was intercalated into the gallery space of MgAl-LDH because of anion exchange between nitrate and salicylate in the reaction solution that was both due to gain in enthalpy and entropy. Nitrate being more hydrophilic and smaller in size would prefer to be solvated in aqueous solution at the expense of salicylate that is more hydrophobic and larger in size and thus going into the interlayer space of MgAl-LDH. Also entropic freedom of water molecule was much more enhanced in presence nitrate in the aqueous solution rather than salicylate. This explains why salicylate would rather prefer to go into the gallery space of LDH with nitrate being released into the aqueous solution.

Figure 7 (a) shows the XRD pattern of Mg-Al LDH synthesized at pH 8. The XRD pattern obtained for as such synthesized Mg-Al LDH nanopowders showed not only characteristic peaks of the LDH material but also showed characteristic peaks of AlO(OH). The planes

(020), (040), (230) marked with (\*) as in figure 7 (a) were found to be the characteristic planes of diasporite  $[\text{AlO}(\text{OH})]$  when compared with a JCPDS ref code [79-1781]. It is clearly visible that apart from LDH, phases of  $\gamma$   $\text{AlO}(\text{OH})$  appeared in the XRD pattern of the as-synthesized powder. The powder prepared at pH lower than 10 contained mixed phases of LDH and  $\gamma$   $\text{AlO}(\text{OH})$ , because of premature precipitation of aluminum hydroxide as compared to mixed aluminum hydroxide and magnesium hydroxide. On aging some fraction of aluminum hydroxide phases separated out from LDH phase to give rise to diasporite that has appeared in the XRD pattern of the synthesized Mg-Al LDH.

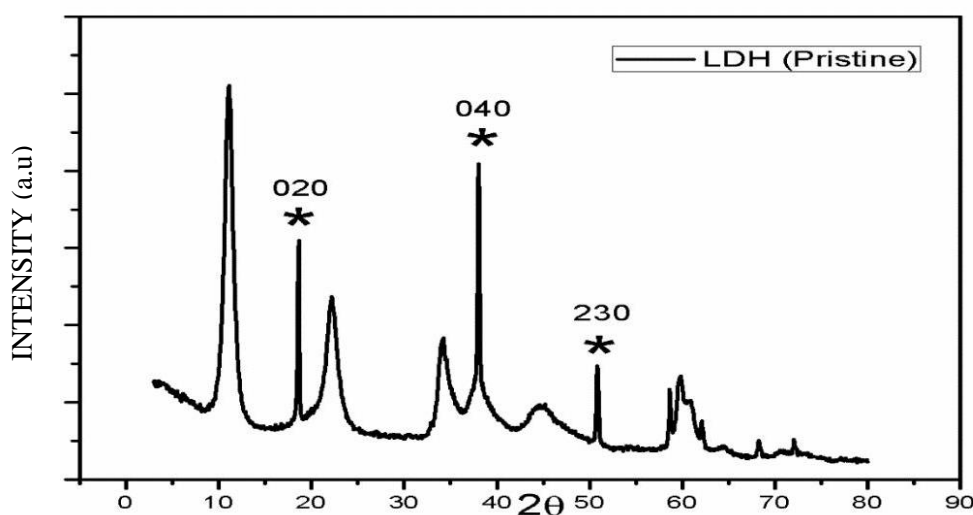


FIGURE7 (a): XRD pattern of Mg-Al LDH nanopowder at pH 8.

As such synthesized Mg - Al LDH powder on heat treatment at 500°C for 2 hours formed metastable phases of Mg and Al oxides. Such heat treated powder on subsequent hydrolysis in an aqueous solution of salicylate exhibited memory effect to reconstruct LDH-SA hybrids with SA intercalated into the interlayer space of LDH. Salicylate intercalation into the interlayer space of Mg Al LDH was confirmed from the shift of (003) plane of LDH to lower angle increasing the  $d_{003}$  to higher value in LDH-SA as compared to pristine LDH as in figure 7(b).

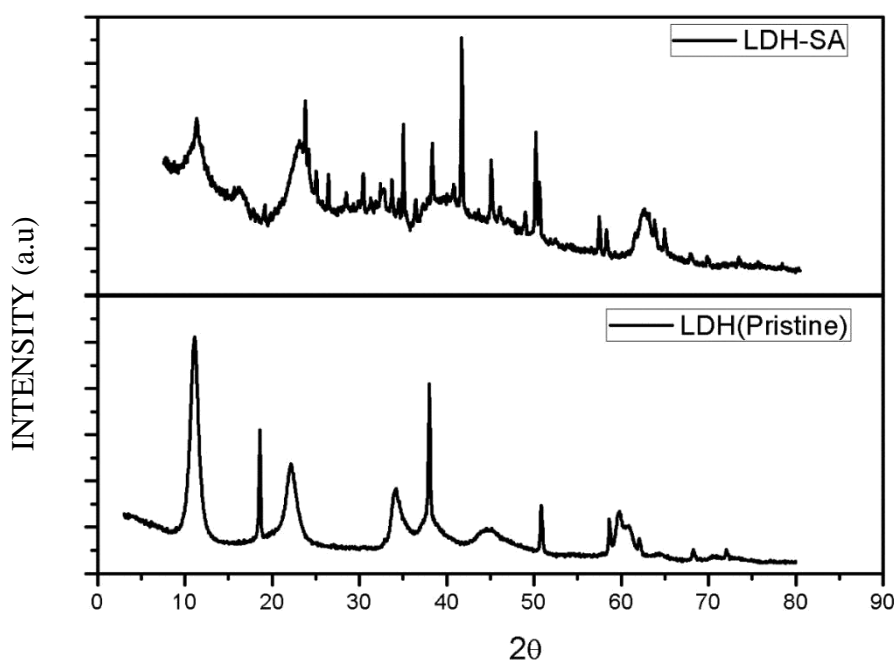


FIGURE 7(b): Comparative study of XRD pattern of Pristine LDH and Salicylate intercalated LDH nanopowder .

But when compared with figure 4(a ),(b), it could be clearly observed that along with characteristic LDH peaks, some additional peaks of different material were present . After heat treatment, LDH forms some metastable phases that in the presence of water again hydrolyzed and reconstructed the LDH phase with intercalation of SA in the interlayer space. Since the starting powder contained some  $\gamma$  -Al -O -OH, on heat treatment, it helped in decomposition of LDH into component metastable oxides and hydroxides. That rehydrolyzed to form different hydroxides of Al and Mg along with retention of some LDH phase in the reconstructed material . Even after intercalation of salicylate into LDH, the material contained mixed phases as seen in figure 7(b) . This can adversely affect the efficiency of LDH -SA nanohybrid as carrier and can go for controlled release of the drug, Thus generally LDH reconstruction method is avoided to intercalate SA into LDH for the purpose of controlled release of the anti -inflammatory drug .

## 5.2 PARTICLE-SIZE ANALYSIS:-

The hydrodynamic particle size of LDH and LDH-SA nanohybrids were determined using Dynamic Light Scattering (DLS) technique. It is known that if the size of particles responsible for photon scattering increases by one order of magnitude, the scattered light intensity increases by about a million times. The algorithm in the size measurement software converts the intensity of photon signal to size.

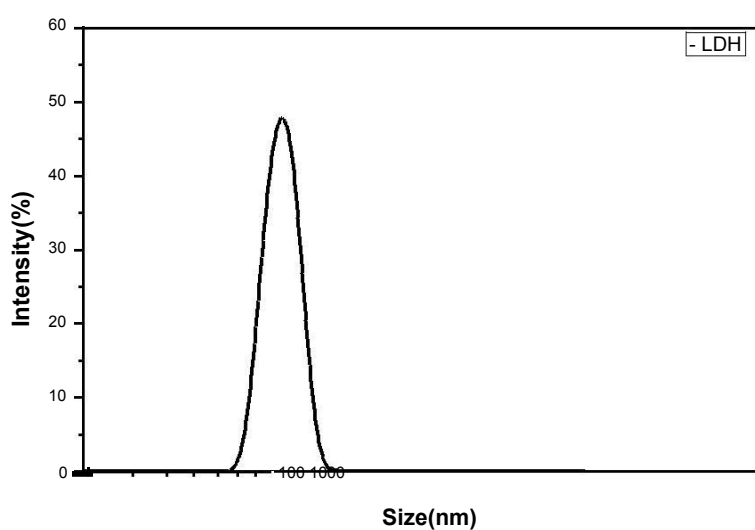


FIGURE 8(a): Particle size distribution of Pristine LDH

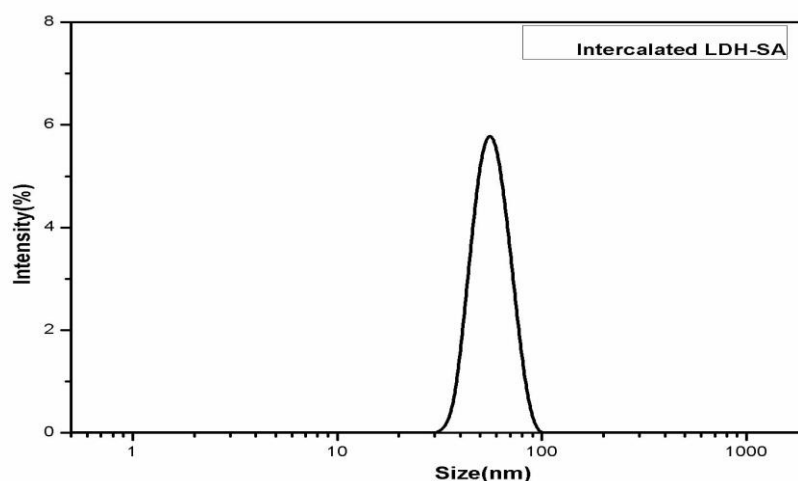


FIGURE 8 (b): Particle size distribution of LDH-SA nanohybrid using coprecipitation method



The aqueous slurry of MgAl - LDH nanoparticles exhibited a particle size distribution between 30 -60 nm, with an average size of 45 nm with a polydispersity index of 0.576 (PDI=0.576) as in figure 8 (a) . The average hydrodynamic particle diameters of LDH -SA nanohybrids synthesized both by coprecipitation and anion exchange methods slightly increased on salicylate intercalation . LDH -SA nanohybrids synthesized using anion exchange method showed narrower particle size distribution (PDI =0.316) with an average particle size of 60 nm . Whereas, LDH - SA nanohybrid exhibited an average particle size of 50 nm (PDI= 0.365), which was synthesized using the coprecipitation method.

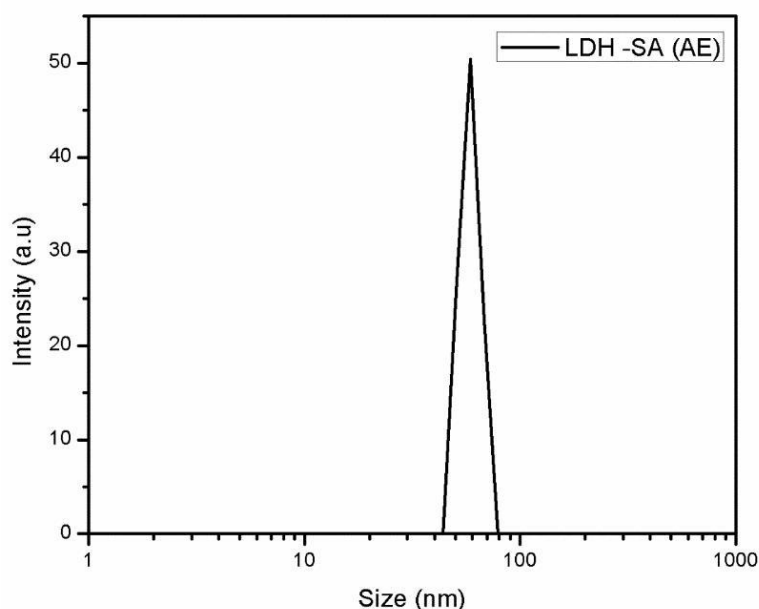


FIGURE 8 (c): Particle size distribution of LDH-SA nanohybrid prepared using anion exchange method.

The majority of the MgAl -LDH– salicylate nanohybrid nanoparticles have particle sizes below 100 nm, which suggests that most of these nanocarriers can escape the reticuloendothelial system (RES) to reach the target cells during drug delivery.

### 5.3 TEM ANALYSIS:-

Transmission Electron Microscopy (TEM) are capable of imaging at a significantly higher resolution than light microscopes, owing to the small de Broglie wavelength of electrons. This enables us to examine the fine details—even as small as a single column of atoms, which is thousands of times smaller than the smallest resolvable object in a light microscope.

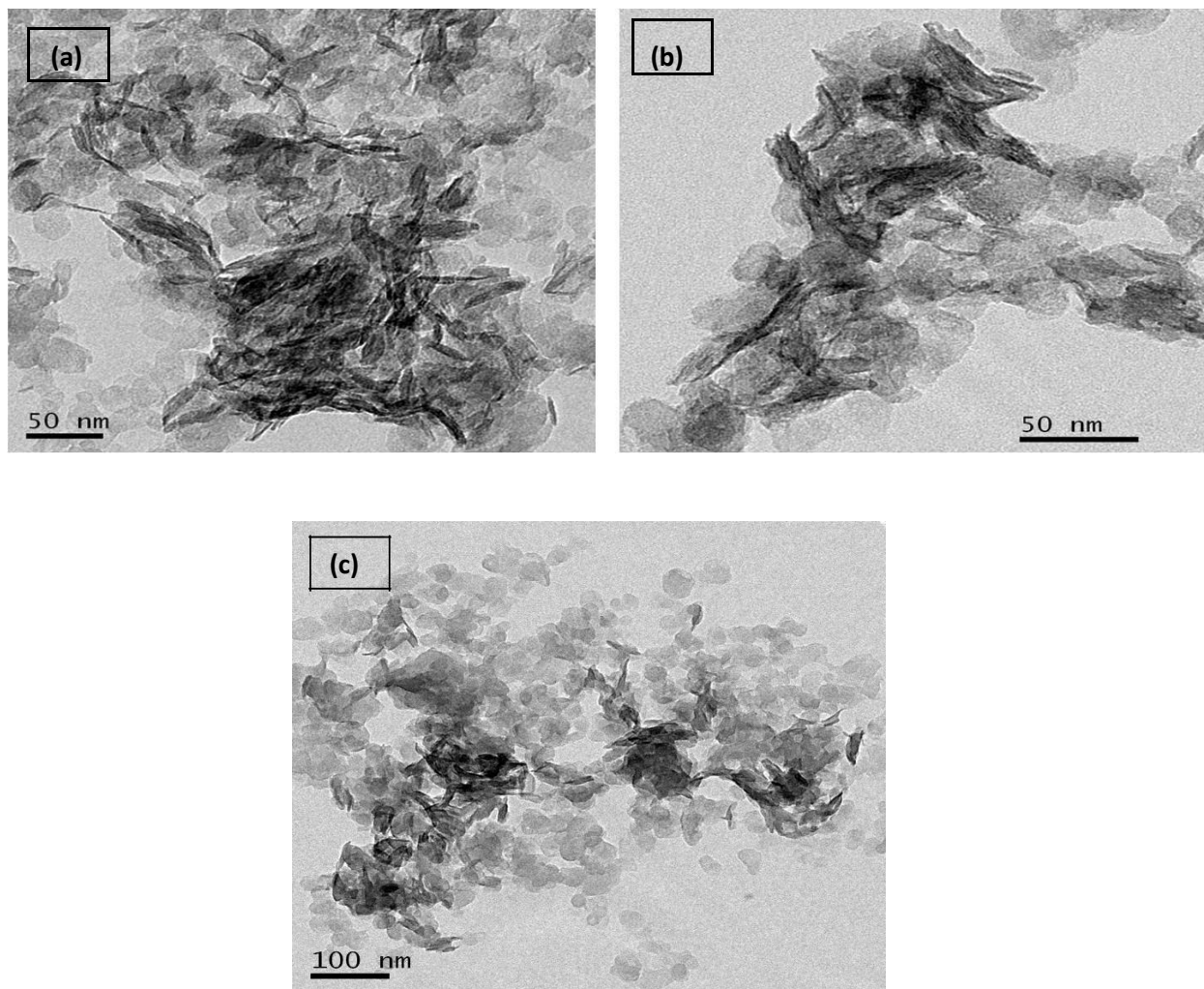


FIGURE 9: TEM micrographs of (a) Pristine LDH (b) LDH - SA nanopowders prepared using co - precipitation (c) LDH - SA prepared using anion exchange

Figure 9 (a), 9 (b) and 9 (c) show the TEM micrographs of pristine LDH and LDH -SA nanohybrid prepared using coprecipitation and anion exchange methods respectively . The morphology of pristine LDH and LDH -SA nanohybrids by coprecipitation method represented the acicular and elongated shape . LDH pristine exhibited a size range between 40 - 60 nm though the intercalated counterpart i . e. LDH -SA nanohybrid showed a little bit higher size range of 50 -80 nm . On the contrary, LDH -SA nanohybrids synthesized using anion exchange process exhibited distinctly different spherical morphology with a size range between 45 -80 nm . The particle size of LDH - salicylate nano hybrid slightly increased as compared to pristine LDH because of intercalation of the drug into the interlayer space . It was found that spherical nanocarriers exhibit better bio -distribution compared to its elongated counterparts during its transport through the blood to target cells. The movement of elongated nanocarriers is little bit hindered through the blood stream and hence it requires greater time to reach the target cells to deliver drugs . As, anion exchange method exhibited better efficiency to intercalate SA molecules into the interlayer space of LDH and also morphologically it is giving better equipped LDH -SA nanohybrids. Our subsequent studies and characterizations would be based on LDH -SA nanohybrids synthesized using anion exchange method .

### **ELEMENTAL COMPOSITIONAL ANALYSIS:-**

Elements	Atomic Percent (%)	
	MgAl LDH	MgAl LDH -SA (AE)
Mg	24.92	19.85
Al	8.25	6.75
O	60.37	47.72
N	5.67	1.26
C	0.78	24.75

**TABLE I:** EDS analysis of LDH and LDH-SA nanopowders synthesized using anion exchange process

From the EDS analysis (Table I) of pristine LDH and LDH – SA nano -hybrid, it is clear that Mg:Al ratio (3.02:1) in the synthesized powder closely resembled with the theoretical composition (Mg: Al= 3:1) . The presence of increased amount of carbon in the LDH - SA nanohybrid powder signified the intercalation of salicylate into the interlayer space of LDH . This result obtained here clearly supports the data as obtained from DSC - TG of the samples bare LDH, sole SA drug and the Mg Al - SA LDH nanohybrid .

## 5.4 FTIR ANALYSIS:-

FTIR analysis is not a diagnostic tool for hydrotalcite, but can prove to be useful to identify the presence of foreign anions intercalated in the interlayer of the brucite-like sheets. Besides that, information about the type of bonds formed by the anions and their orientations can also be detected by this spectroscopy. The FTIR spectra of pristine LDH, SA molecule, and LDH–SA hybrids are shown in the following Figure 10.

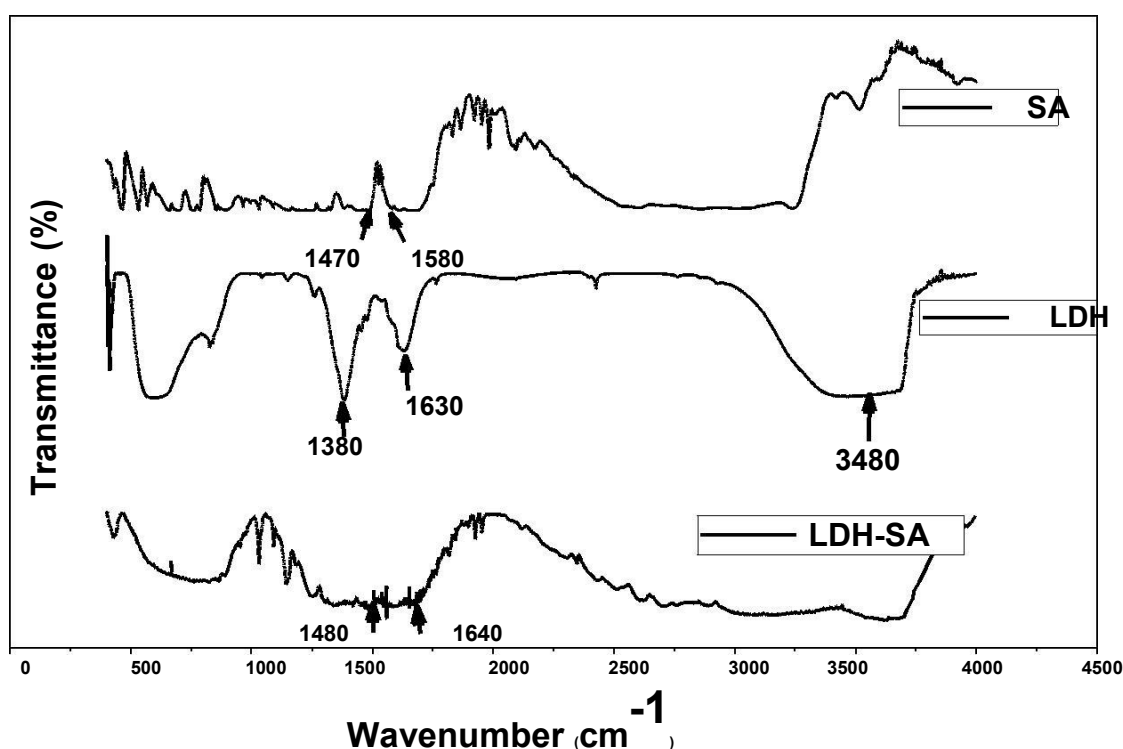


FIGURE 10: FTIR Spectroscopy of Pristine LDH, LDH-SA, Salicylic Acid powder

Two bands at 600 and 428  $\text{cm}^{-1}$  attributed to the lattice vibrations of metal–oxygen and metal–hydroxyl bonds. The presence of bands in 200–1000  $\text{cm}^{-1}$  region are attributed to the vibrations of the anions, and whereas some are related to cation–oxygen vibration. The absorption band at 3480  $\text{cm}^{-1}$  signifies the stretching vibration of the labile hydroxyl group or physically adsorbed water molecule in the brucite-like layer of Mg–Al–LDH [4]. Serna et al.

[5] showed that both the hydrogen stretching and bending frequencies in the hydrotalcite increase as the M(II)/M(III) ratio increases from 2 to 3. This shift correlated with the modification in the layer spacing; moreover, it was observed that the half-width was smaller in the Mg/Al= 2/1 ( $x= 0.33$ ) hydrotalcite, thus suggesting a more ordered cation distribution inside the brucite-like layer. A shoulder was present around  $3000\text{ cm}^{-1}$ ; which attributed to hydrogen bonding between  $\text{H}_2\text{O}$  and the anion in the interlayer water, bending vibration also occurs at  $1600\text{ cm}^{-1}$ . The intensity of these latter two bands depends on the type of anion and the amount of water in the LDH. The presence of a strong band at  $1384\text{ cm}^{-1}$  signifies the existence of  $\text{NO}_3^-$  anions in MgAl-LDH structure [6].

In most cases of hydrotalcite-like material the bands observed at  $1350\text{-}1380\text{ cm}^{-1}$  ( $\nu_3$ ),  $850\text{-}880\text{ cm}^{-1}$  ( $\nu_2$ ) and  $670\text{-}690\text{ cm}^{-1}$  ( $\nu_4$ ), as well as in some cases the presence of a shoulder around  $1400\text{ cm}^{-1}$ , or of a double band in the region  $1350\text{-}1400\text{ cm}^{-1}$  [7], attributed to lowering of the symmetry of the carbonate (site of symmetry  $\text{C}_{2v}$ ). It also attributed to the disordered nature of the interlayer [7,5], which subsequently caused the removal of the degeneracy of the  $\nu_3$  and  $\nu_4$  modes. The lowering of the symmetry also causes the activation of the  $\nu_1$  mode at around  $1050\text{ cm}^{-1}$ . Miyata [8] explained the observed lowering of symmetry by hypothesizing two different kinds of carbonate anion coordination; existing in the interlayer region as a monodentate or a bidentate complex. The author had also reported the same explanation to justify the band splitting in some hydrotalcite containing different anions [ $(\text{NO}_3)^-$ ,  $(\text{SO}_4)^{2-}$ ,  $(\text{ClO}_4)$ ] [8,9]

Serna et al. [10] explaining differently, hypothesized that the bands observed at  $1625\text{ cm}^{-1}$  could be related to the presence of bicarbonate ions, whereas the splitting of the band around  $1380\text{ cm}^{-1}$ , as well as the appearance of the band at  $1060\text{ cm}^{-1}$ , related to a perturbation of the carbonate anion under vacuum.

The presence of several functional groups in the salicylic acid gave rise to a spectrum with many absorption bands. The band attributable to  $\text{C=O}$  vibration of the acid has vanished

because the salicylic acid was intercalated in the anionic form inside the LDH. Intense bands have been found to develop at  $1566\text{ cm}^{-1}$ ,  $1453\text{ cm}^{-1}$ , and  $1348\text{ cm}^{-1}$  that attributed to the asymmetric and symmetric carboxylate stretching mode of the salicylate anions.[11,12].In addition to bands at high wave number values due to  $\nu(\text{OH})$  and  $\nu(\text{=C-H})$  moieties, a band was recorded at  $1658\text{ cm}^{-1}$  due to mode  $\nu(\text{C=O})$  of the acid group. The abnormally low value for the position of this band was due to intramolecular hydrogen bonds. The bands due to  $\nu(\text{C-C})$  of the aromatic ring were assigned to  $1605$ ,  $1484$ , and  $1467\text{ cm}^{-1}$ . While those due to modes  $\nu(\text{C-O})$  and  $\delta(\text{O-H})$  of the acid and alcohol functions were recorded at  $1441$  and  $1290\text{ cm}^{-1}$  respectively. The In-plane and out-of-plane  $\delta(\text{CH})$  bands were recorded below  $1000\text{ cm}^{-1}$ [13]. Peaks at  $1573$  and  $1376\text{ cm}^{-1}$  attributed to the  $\nu_{\text{as}}$  and  $\nu_{\text{s}}$  vibration of  $\text{COO}^-$ . After the ion-exchange reaction, the  $\nu_{\text{as}}$  and  $\nu_{\text{s}}$  absorption peaks of  $-\text{COO}^-$  moved to  $1608$  and  $1432\text{ cm}^{-1}$  respectively. These results indicated the presence of strong electrostatic interactions between the cationic host layers and the salicylate anions [12,14].

## 5.5 THERMAL ANALYSIS:-

LDHs are reactive materials that undergo endothermic decomposition producing water and metal oxide residue. This property could be useful in improving the thermal stability and flame-retardance of polymer matrix more efficiently. The thermal behaviour of the hydrotalcite material generally characterized by two transitions: firstly, endothermic at low temperature which corresponds to the loss of interlayer water, without the collapse of the structure; this step is reversible [15]. And secondly, endothermic, at a higher temperature that is due to the loss of hydroxyl groups from the brucite-like layer, as well as of the anions. These two transitions depend quantitatively and qualitatively on many factors, such as: M(II)/M(III) ratio, the type of anions, low temperature treatment (hydration, drying, etc), and the heat treatment atmosphere.

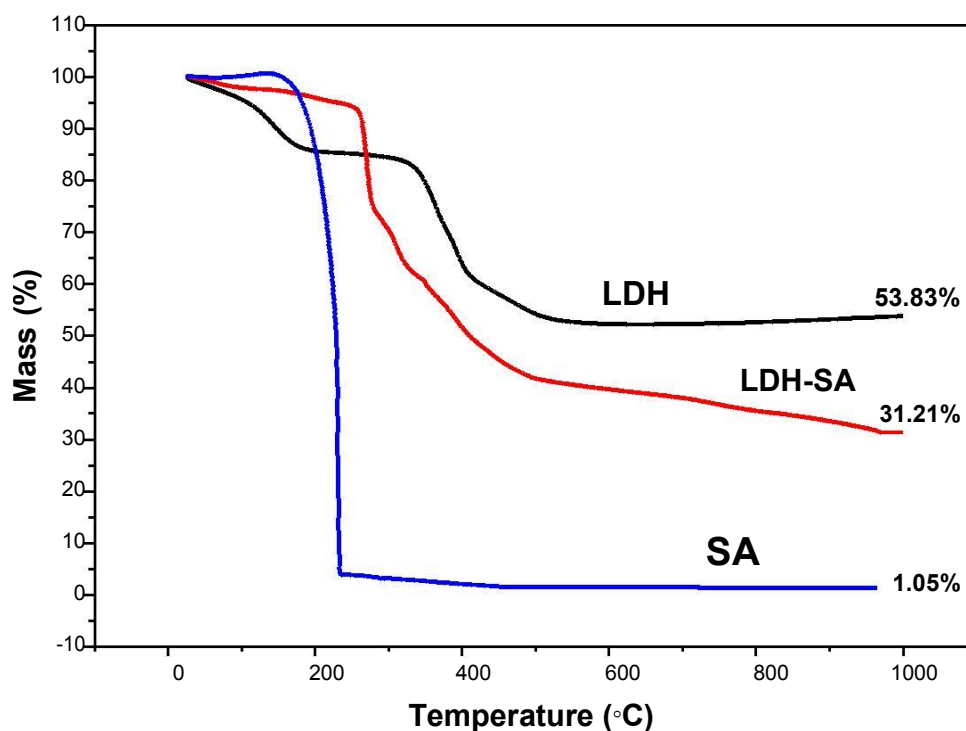


FIGURE 11 (a): Thermogravimetric plot of LDH, SA, LDH-SA nanopowders



Thermogravimetric curves (TG), carried out on LDH, SA, and LDH-SA under air purge (thermo-oxidative analysis), are shown in Figure 11(a). The Mg Al-LDH powder showed a typical thermogram of hydrated product losing 46.17% of its mass on heating till 1000 °C. On the other hand, the salicylate intercalated LDH powders exhibited a mass loss of about 68.69%. Considering, the fact that SA fully decomposed within this temperature range, the amount of SA intercalated into Mg Al LDH was found to be 22.5%. The mass loss in Mg-Al LDH was spread over three major regions as evident from the TG-DTA plot in Figure 11 (a,b).

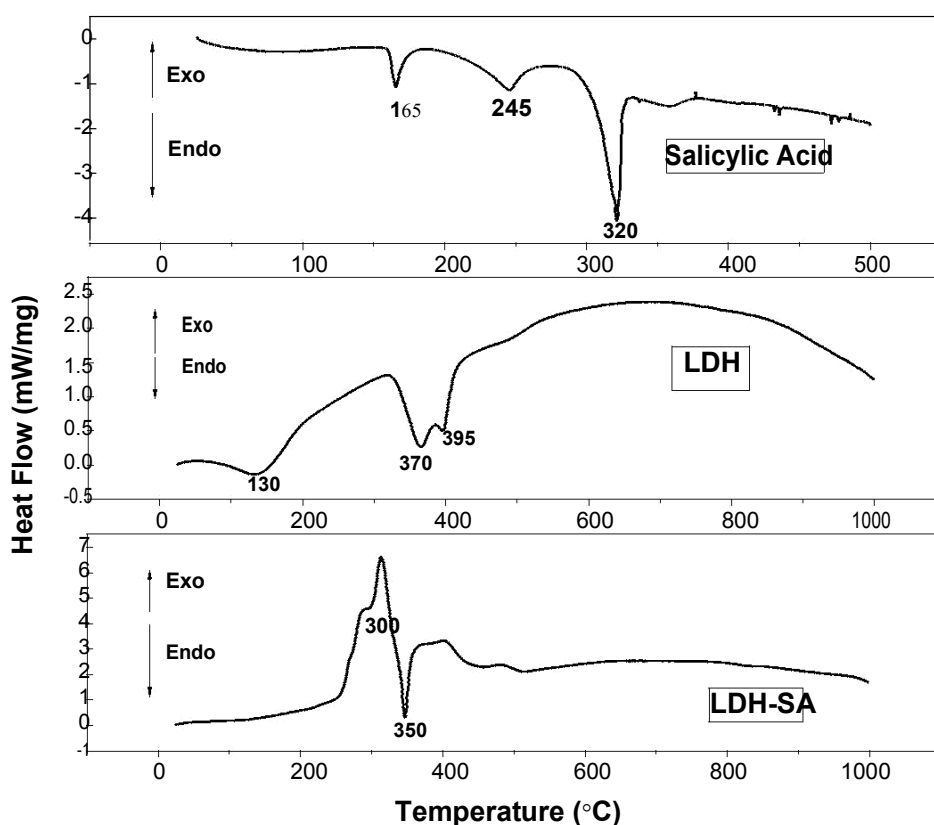


FIGURE 11(b): Differential thermal analysis (DTA) of LDH, SA and LDH-SA nanopowders.

The first endothermic peak at 130 °C was due to the removal of adsorbed moisture. This followed by the double endothermic effects at 370 and 395 °C, which contribute to the loss of interlayer water and charge balancing interlayer nitrate ions respectively.

The lower mass loss at higher endothermic temperatures (510 °C) attributed to the dehydroxylation and decarboxylation process leading to the conversion of the LDH into  $\text{MgAl}_2\text{O}_4$  spinel. The interesting shift in decomposition temperature of salicylate due to endothermic shift from 320 °C to 350C attributed to the higher thermal stability of salicylate in the interlayer space of LDH as compared to its free state.

## 5.6 FESEM ANALYSIS:-

Field emission scanning electron microscopy (FESEM) provides a topographical and elemental information at magnifications of 10x to 300,000x, with virtually unlimited depth of field. When compared with conventional scanning electron microscopy (SEM), field emission SEM (FESEM) produces clearer, less electrostatically distorted images with spatial resolution three to six times better.

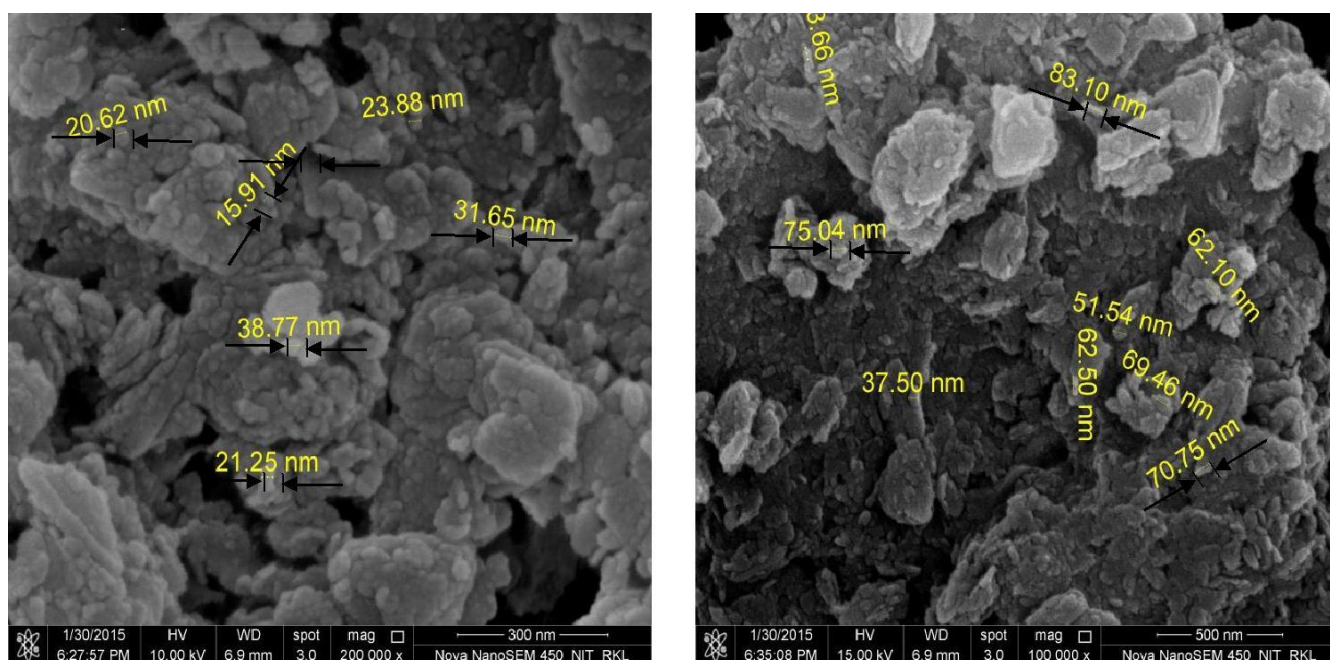


FIGURE 12: FESEM analysis of (a) Mg-Al LDH nanopowder (b) Mg-Al LDH-SA nanohybrid.

The average particle size of the Mg-Al LDH nanopowder as observed from figure 12 (a) was found to be around 20-40 nm. Whereas on the other hand the average particle size of the Mg-Al LDH-SA nanohybrid nanopowder was estimated to be around 30-80 nm as in figure 12 (b). Since the increase in the average particle size of the intercalated nanopowder is clearly evident from the figure 12 (b). So it strongly supports the fact that salicylate intercalation into the interlayer space of the Mg-Al LDH nanopowder caused expansion of crystal lattice.

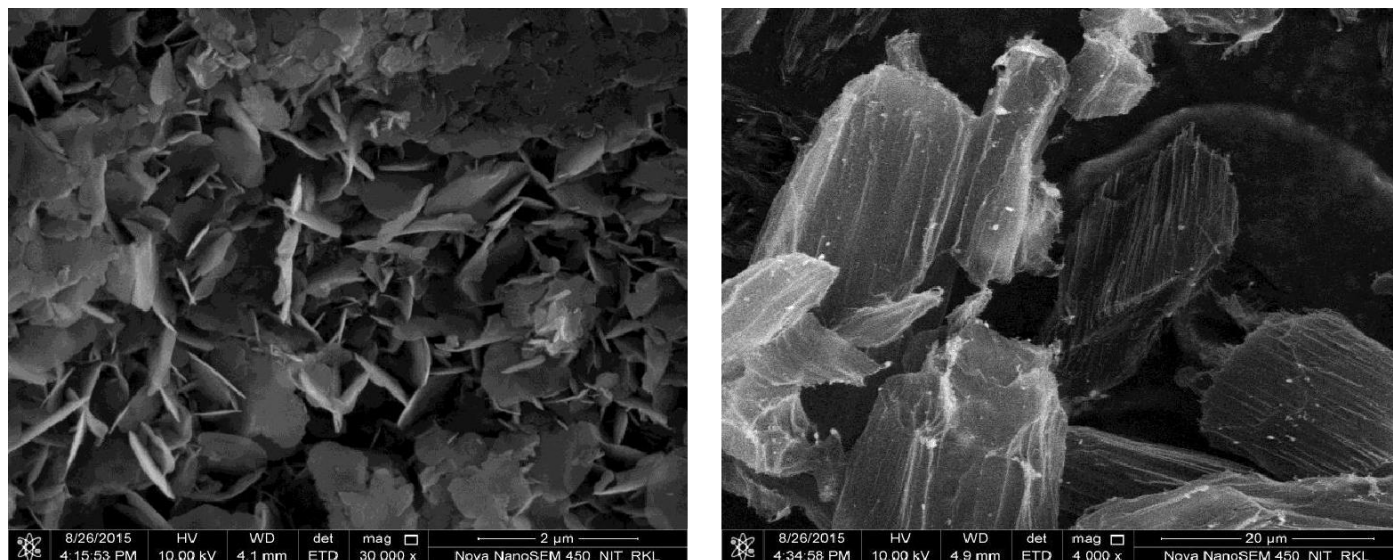


FIGURE 13: FESEM analysis of (a) Heat – treated Mg-Al LDH nanopowder (b) Mg-Al LDH-SA reconstructed nanohybrid.

Since from figure 13 it can be clearly said that the average particle size of , both the pristine Mg-Al LDH nanopowder and the salicylate intercalated LDH nanohybrid increases on being heat treated. So heat treated material in case of controlled release of Layered Double Hydroxide won't be a very suitable idea.

The calcined Mg-Al LDH powder showed nanoplatelet like morphology. The 500°C calcined Mg-Al LDH powder on reconstruction in the presence of an aqueous solution of Salicylate, formed Salicylate intercalated Mg-Al LDH. Though LDH-SA powder on drying formed agglomerated platelets and bands of assembled platelets is clearly visible in SEM micrographs in figure 13 (b). The average particle size Of LDH and SA-LDH nanohybrid increased due to crystal growth and agglomeration due to calcinations at 500°C. So, it can no longer escape the Reticulo Endothelial System (RES) to avoid phagocytosis. Thus, the powders are suitable for carrying the drug through the blood to specific sites of the body.

## 5.7 CHN ANALYSIS:-

A **CHN Analyzer** is a scientific instrument that determine the elemental composition of a sample. The name derives from the three primary elements measured by the device: carbon (C), hydrogen (H) and nitrogen (N). Sulfur (S) and oxygen (O) can be also measured. Such analyzers usually use very small quantities, many times around 1 to 3 mg of the sample. The analyzer uses a combustion process to break down substances into simple compounds that are then quantified, usually by infrared spectroscopy.

Element	Content (%)	
	LDH	LDH-SA (AE)
C	0.39	16.06
N	5.21	2.16
H	2.28	3.59

**TABLE II:** CHN analysis of LDH and LDH-SA nanopowders

The CHN analysis of MgAl-LDH and MgAl-LDH-SA are given in Table II. The amount of SA intercalated into the interlayer space of MgAl-LDH was found to be 263.84 mg of SA/g of LDH-SA. This corresponds to approximately 26.4wt% SA in the LDH-SA formulation, which is in close agreement with data obtained from the thermogravimetric analysis.

## 5.8 IN-VITRO DRUG RELEASE:-

The salicylate release profile from the LDH matrix at physiological pH (7.4) at a constant temperature of 37.1°C was evaluated in the phosphate buffer solution using a UV-visible spectrophotometer.

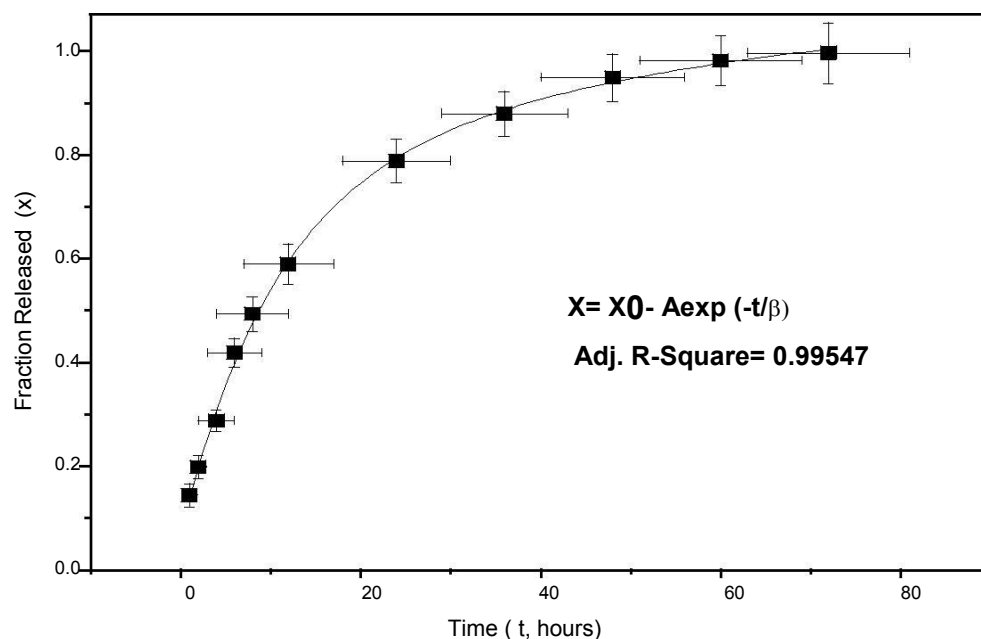


FIGURE 14: Release kinetics of SA from LDH-SA in PBS (pH-7.4) at 37 °C.

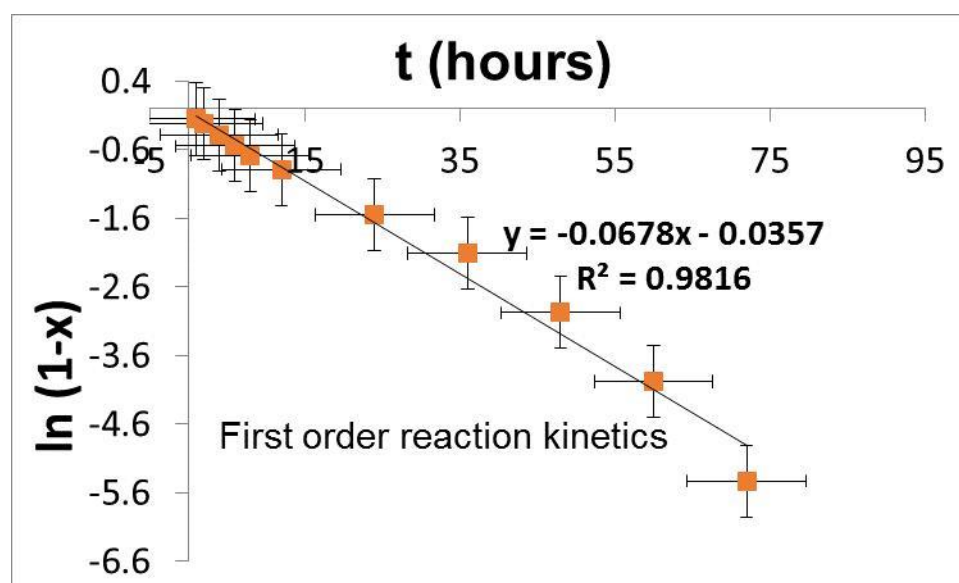


FIGURE15: Fit of first order release kinetic data to observed release rate

The release of the drug up to 20 hours followed a faster kinetics though no burst release was observed at the beginning of the release tests. This phenomenon primarily attributed to the release of loosely bound SA molecules from the edges of interlayer spaces and free surfaces followed by subsequent release of salicylate anion from the interlayer space of LDH due to de-intercalation. The later stage of slower release (after 20 hours) of salicylate governed by a combination of drug diffusion and LDH dissolution. The release profile shows that ~50% of the incorporated salicylate was released in 16 hours, and it increased nonlinearly to ~80 % in 30 hours. The entire amount (~99%) of salicylate was released within the time frame of 72 hours that clearly showed the ability of LDH in controlled and sustained drug release. The cumulative release (%) of salicylate was nonlinear with respect to elapsed time and exhibited an exponential release rate as given in Figure 14.

$$X = M_t / M_{\infty} = X_0 - A \exp(-t/\beta) \dots\dots\dots(1)$$

Where  $X_0 = 0.9753$ ,  $A = -0.8946$  and  $\beta = 14.023$  in this case.

$$X = 1 - \exp[-k(t - \alpha)] \dots\dots\dots(2)$$

$$X = k(t - \alpha)^{0.5} \dots\dots\dots(3)$$

$$X = k t^n \dots\dots\dots(4)$$

$$X = k(t - \alpha)^n \dots\dots\dots(5)$$

where  $X$ ,  $t$ ,  $k$ ,  $\alpha$  and  $n$  are the fraction of drug release, release time, kinetics constant, modified parameter and an exponent respectively.

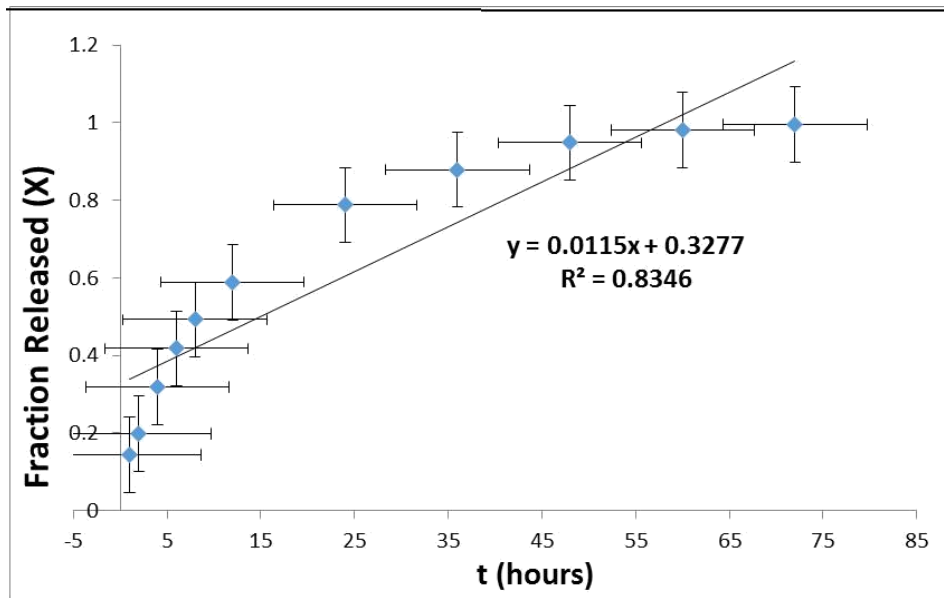


FIGURE 16: Release kinetic fitted to zero order reaction kinetic

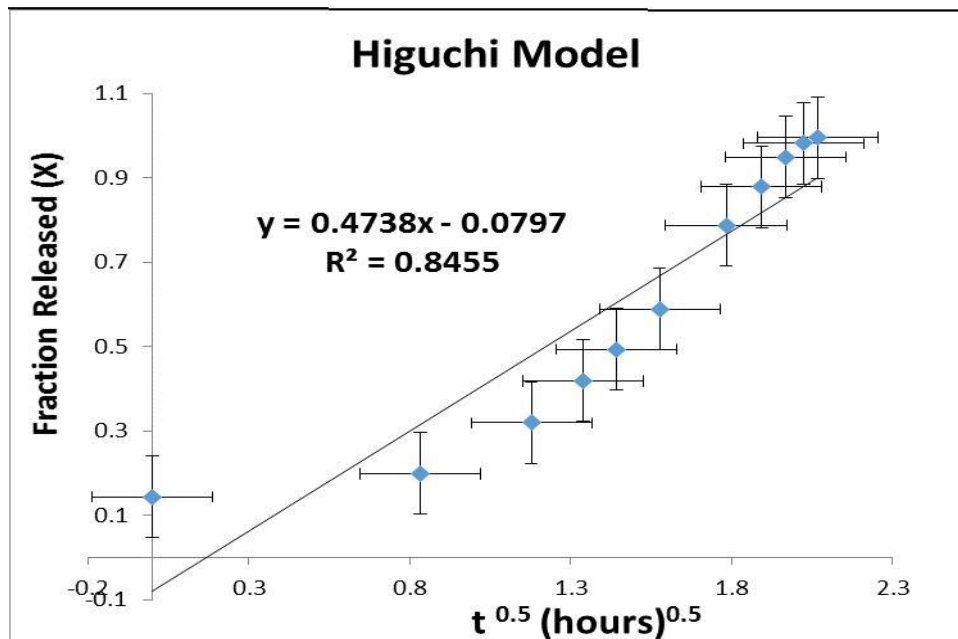


FIGURE 17: Release kinetic fitted to Higuchi model



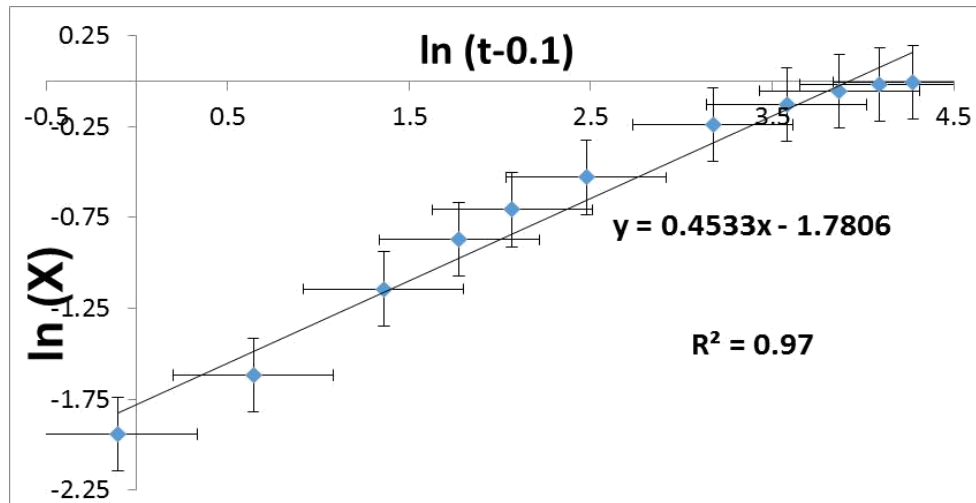


FIGURE 18: Release kinetic fitted to Rigter- Peppas model

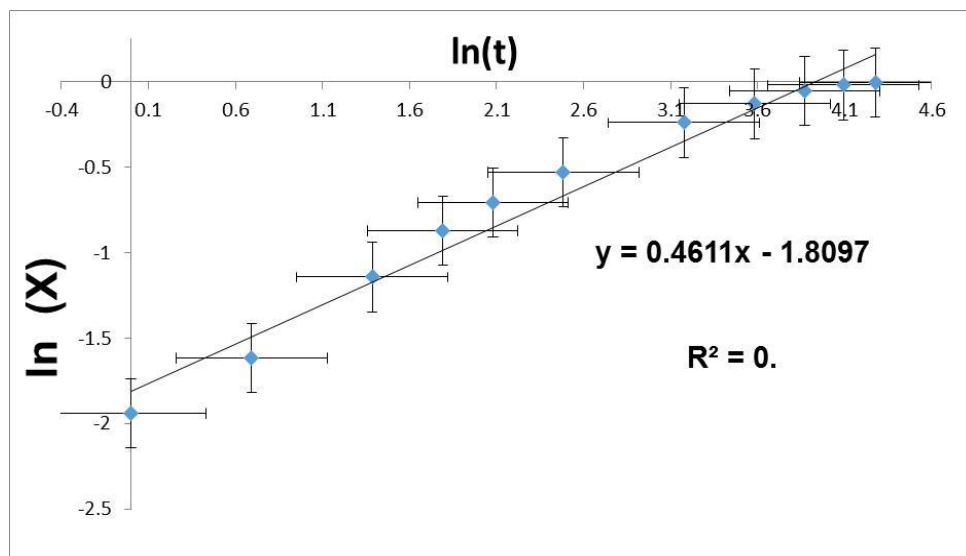


FIGURE 19: Release kinetic fitted to Korsmeyer- Peppas model

The SA release data was fitted to zero-order[19] [Figure 14], first-order [Eq.(2)] [20], Higuchi (Eq.(3)[20,21] [Figure 17], Rigter–Peppas (R–P) model [Eq.(5)] [20] [Figure 18], and Krosmeier- Peppas [Eq (4)] [22] [Figure 19] to investigate the release dynamics of this system.

Sample	Zero Order $R^2$	First Order $R^2$	Higuchi $R^2$	Korsmeyer- Peppas Model		Rigter- Peppas Model	
				$R^2$	n	$R^2$	n
LDH-SA	0.8346	0.9816	0.8455	0.97	0.4611	0.9729	0.4533

TABLE III: Drug release kinetic parameters derived from UV- visible spectrophotometer

Release exponent	Drug Transport Mechanism	Rate as a function of time
0.5	Fickian Diffusion	$t^{-0.5}$
$0.45 < n = 0.89$	Non Fickian transport	$t^{n-1}$
0.89	Relaxational Transport	Zero Order Kinetics
$>0.89$	LDH dissolution	$t^{n-1}$

TABLE IV: Interpretation of diffusional release mechanisms from LDH- SA nano hybrid.

The derived fitting parameters of  $\alpha$ , n and R are given in Table III. The exponent n is normally used to describe different release mechanisms as shown in Table IV. The fitting results of drug release profiles on the basis of the first order release kinetics model are shown in the figure15. It is evident that the SA drug release from LDH followed first order release kinetics with a satisfactory coefficient of 0.9816. This was also followed by Rigter –Peppas (R-P) model of release kinetics (Table III) with a fitting coefficient of 0.9729. The value of n is 0.4533 ( $0.45 < n < 0.89$ ) in R–P model at pH 7.4 indicates that SA drug release mechanism from Mg-Al LDH controlled by the non- Fickian transport mechanism. Which is a combination of diffusion and LDH dissolution in physiological solution [19,20], that is closely relevant to first order release kinetics.

## **5.9 DISSOLUTION STUDY USING ATOMIC ABSORPTION SPECTROSCOPY:**

Atomic absorption spectroscopy (AAS) is a spectro-analytical procedure for the quantitative determination of chemical elements using the absorption of optical radiation (light) by free atoms in the gaseous state. This technique makes use of absorption spectrometry to assess the concentration of an analyte in a sample. It requires standards with known analyte content to establish the relation between the measured absorbance and the analyte concentration and relies therefore on the Beer-Lambert Law.

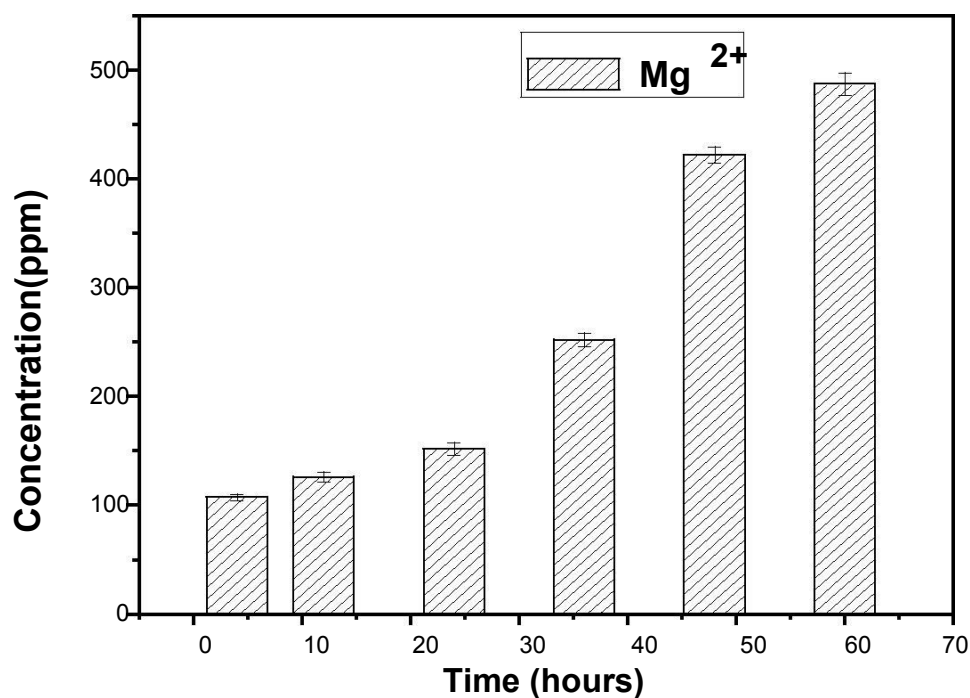


FIGURE 20: Dissolution kinetic of Mg-Al LDH in PBS of pH 7.4

The kinetic dissolution data for Mg-Al LDH in figure 20 shows that significant degree of dissolution was observed in LDH immersed in PBS solution of pH 7.4 within 4 hours of

immersion time. After 30 hours, the rate of dissolution of MgAl LDH at pH 7.4 became significantly higher and increased continuously after that up to 60 hours. At initial stages, the dissolution of surface layers of LDH may not influence the drug release kinetics. After 30 hours, the rate of LDH dissolution was high enough to cause disintegration of intercalated structure of LDH to release drug molecules. Atomic absorption spectroscopy data in figure 20 clearly suggests that dissolution of MgAl LDH into PBS of pH 7.4 played a vital role in determining its salicylate release behaviour particularly at the later stages, after 30 hours of incubation in PBS.

## 5.10 **HEMOCOMPATIBILITY ANALYSIS:-**

Hemocompatible materials are those substances that cause no negative influence on blood. Blood represents one of the most complex biochemical systems in living organisms. Its various components play integral roles in several life functions, including the transport of oxygen, destruction of invading pathogens, and repair of damaged tissue. Medical devices that contact blood during routine use must be hemocompatible. That is, they must not adversely interact with any blood components so as to cause their inappropriate activation or even destruction. Blood is composed of a multitude of cell types, ranging from simple oxygen-carrying erythrocytes to sophisticated antigen-specific lymphocytes. The various cells participate in a vast array of functions, including tissue repair and immune responses as well as oxygen transport. Because of the range and criticality of these functions, any source of cytotoxicity to blood cells can cause significant harm. Most significantly for example hemolysis, the breakdown of red blood cells, which can be material-mediated or result from mechanical damage and directly impairs the ability of the circulatory system to carry oxygen to body tissues. Likewise, adverse interaction with white blood cells can impair the body's ability to eliminate invading pathogens efficiently. Blood also contains several soluble multicomponent protein systems that systematically interact in various ways to perform critical functions, like the complement system participates in inflammatory reactions and facilitates removal of invading pathogens. Similarly, the clotting cascade operates to initiate coagulation, thereby preventing excessive loss of fluid and facilitating tissue repair. Inhibition of either of these cascade systems can have significant adverse effects on the body. Therefore, a structured test -selection system is performed primarily based on clinical concerns.

The hemocompatibility tests were performed for the layered double hydroxide samples as per the American Society for Testing and Materials (ASTM) standard protocol, which figures out

the extent of hemolysis in the presence of samples. Here for the tests to perform fresh goat blood was collected in the presence of Tri Sodium Citrate (TSC) in the proportion of 3.8 gm of TSC per 100 ml of blood to prevent the coagulation of blood vessels. The citrated blood thus obtained was then diluted with normal saline in the ratio of 8:10 (blood: saline). Then 0.5 ml of diluted blood is taken in a centrifuge tube

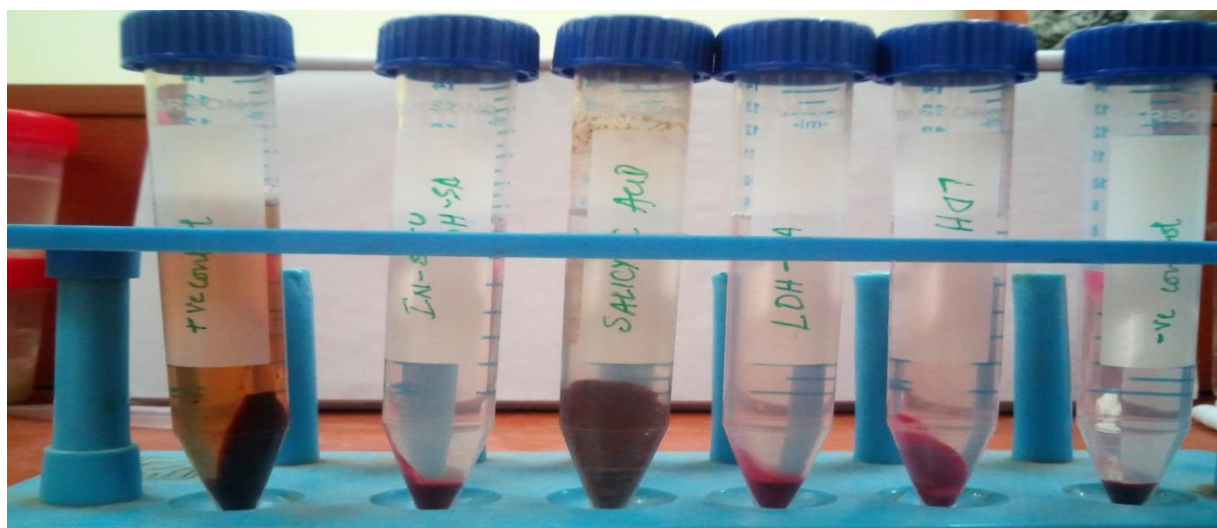


FIGURE 21 : Samples prepared for the hemolysis test.

### **Results obtained:-**

TABLE V: The OD values obtained after the hemocompatibility test for LDH, SA, LDH-SA nanohybrid

	+ve (control)	-ve (control)	LDH	LDH-SA (AE)	SA
OD values	0.324	0.104	0.115	0.113	0.116

TABLE VI: Percentage Hemolysis for the three samples against the OD values.

	LDH	LDH-SA (AE)	SA
% Hemolysis	5.0	4.2	5.5

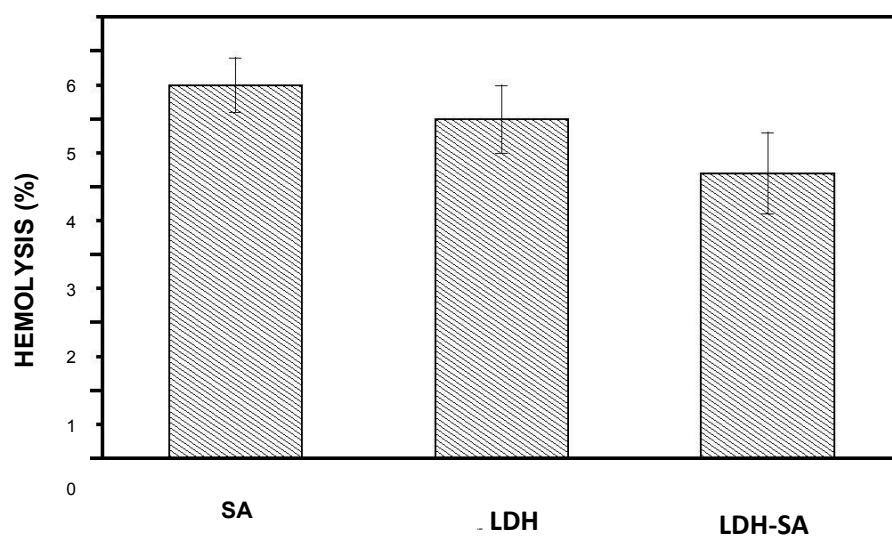


FIGURE 22: Percentage hemolysis of free SA, LDH, and LDH –SA nanohybrid.

From figure 22, it is visibly clear that all the samples were hemocompatible. The ceramic nano- powder LDH (pristine) having a hemolysis percentage value of 5, indicated that the sample is hemocompatible with blood cells of the body. The sole drug-free salicylic acid with a percentage hemocompatibility of 5.5 attributed to the fact that it is not highly hemocompatible but is mildly compatible with the blood cells of the body. The intercalated sample Mg-Al LDH-SA nanohybrid showed percentage hemolysis of 4.2. Thus, it clearly indicates high hemocompatibility of LDH-SA with the blood cells. That means, SA in intercalated of LDH is more hemocompatible than the free salicylic acid.

### 5.11 **MTT ASSAY ANALYSIS:-**

The term MTT assay refers to a colorimetric assay used for assessing cell metabolic activity.

The cytotoxicity of the synthesized material was determined using the MTT assay. These are cell viability, and cytotoxicity assays used for drug screening and cytotoxicity tests of chemicals. Various reagents are being used for cell viability detection,

based on various cell functions such as enzyme activity, cell membrane permeability, cell adherence, ATP production, co-enzyme production, and nucleotide uptake activity. MTT assay measures the reduction of yellow 3-(4, 5-dimethylthiazol- 2-yl)-2,5-diphenyl tetrazolium bromide (MTT) by the enzyme mitochondrial succinate dehydrogenase.

The cell line used for measuring MTT assay of Mg-Al LDH were HEK 293, popular for their ease of growth and transfection. HEK293 is a cell line derived from human embryonic kidney cells grown in tissue culture. They are also known, more informally, as HEK cells. The MTT enters the cells and passes into the mitochondria where it reduces to an insoluble, colored (dark purple) formazan product. The insoluble purple colored formazan are then solubilized with an organic solvent (e.g., isopropanol) and the color intensity released, solubilized formazan reagent is measured spectrophotometrically . Since the reduction of MTT can only occur in metabolically active cells the level of activity is a measure of the viability of the cells. Below is the reaction of MTT being converted to Formazan on treatment with mitochondrial reductase.





MTT assay was thus performed using HEK 293 cell lines cultured in the MEM & FBS media. It was found all materials, were mildly toxic towards the cells. Pure ceramic nanoparticle Mg-Al LDH was found to be least toxic as when compared with the free Salicylic Acid sample and the Mg-AL LDH-SA nanohybrid. From the plot, it is clearly visible that cell viability (%) of salicylic acid increased with decreasing concentration of the sample being introduced into the cells. SA intercalated LDH (LDH-SA) followed the same trend.

Cell viability in contact with free SA increased from 70 % at 25  $\mu\text{g/ml}$  to 95% at a lower concentration of 1.562  $\mu\text{g/ml}$ . Similarly the cell viability of the LDH-SA sample (i.e. the nanomaterial intercalated with the drug salicylic acid) increased from 85% at 25  $\mu\text{g/ml}$  to almost 99% at 1.562  $\mu\text{g/ml}$ . It clearly attributed that higher concentration (25  $\mu\text{g/ml}$ ) of LDH-SA imparts a condition that is more cytotoxic that indicated a cell viability of 85% .Whereas when the concentration of the sample decreased to 1.562  $\mu\text{g/ml}$ , the cell viability increased to 99 %, making it more conducive to cell growth and proliferation. Since the number of viable cells were more in the presence of the same amount of SA intercalated LDH sample as compared to the free SA, the drug intercalated inside LDH exhibited lower cytotoxicity. In spite of the samples being non-toxic no conclusive effect of concentration on cell viability could be drawn from these test results. Exposure to a higher concentration of the test samples for prolonged duration were probably required for the determination of an IC 50 value for each of the test samples. This would be required to obtain more comprehensive information on the effect of test materials on cell viability of the samples. On the basis of which the effect of the nanohybrid material could be carried out at the molecular level. Thus, it can be said that SA in an intercalated form inside the LDH nanomaterial is less cytotoxic to human kidney cells in comparison to the bare drug itself.

## 5.12 DNA FRAGMENTATION ANALYSIS:-

DNA fragmentation is the separation or breaking of DNA strands into pieces. It can be done intentionally by laboratory personnel or by cells, or can occur spontaneously. Spontaneous or accidental DNA fragmentation is molecular fragmentation that gradually accumulates in a cell. It can be measured by e.g. the Comet assay. Here the analysis of DNA fragmentation was performed using agarose gel electrophoresis method after culturing HEK 293 [Human Embryonic Kidney cells] cell lines in the presence of samples. The cells were first of all retrieved in a mixed solution of MEM [Minimum essential media (45 ml)] along with 10 % FBS [Foetal Bovine Serum (5ml)] media. The stored cells are thus mixed with the media and attached to the surface of the flask in which the cells were seeded when they were grown. The cells were thus kept in the media for 24 hrs to study their nature of growth.

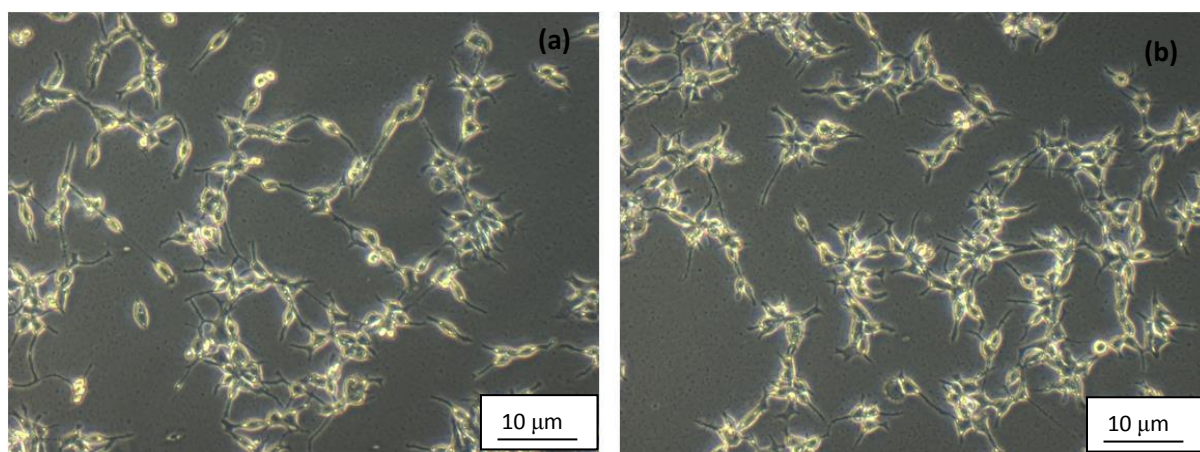


FIGURE 25: Effect of MEM + FBS media on the HEK 293 cells

The microscopic images of HEK 293 cells in figure 25 shows the effect of sole DMEM media on the HEK 293 cells after 24 hours of culture. The cells are looking very healthy with micro extensions on the substrate. The three samples Mg-Al LDH nanoparticle, bare salicylic acid, and the Mg-Al LDH-SA nanohybrids were taken for the treatment of these cells to study

the DNA fragmentation analysis. 0.1mg /mL of each of these samples were taken for the study.

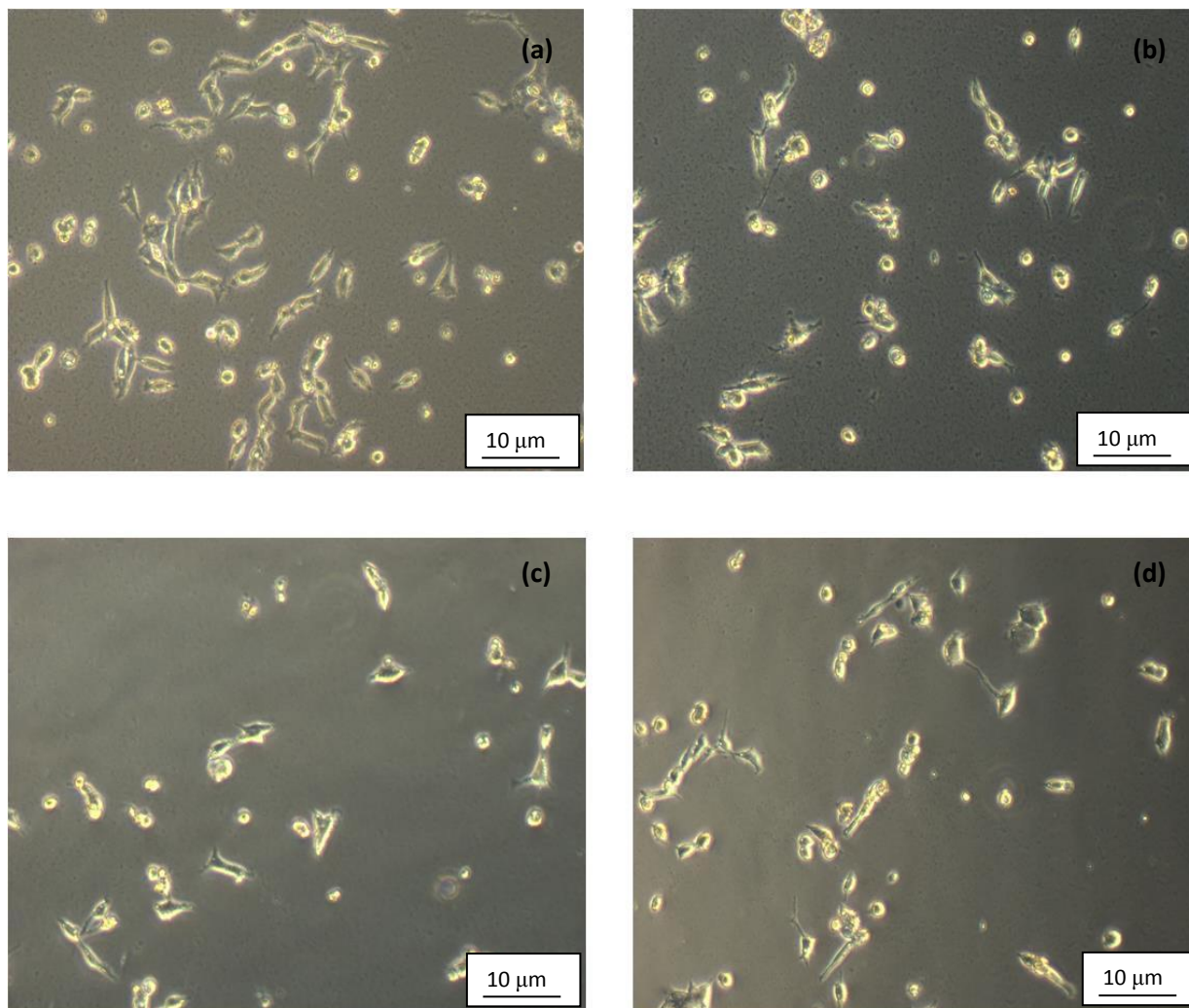


FIGURE 26: Effect of (a) Media (control) (b) LDH (c) SA (d) LDH-SA on the HEK 293 cells after 24 hrs of treatment

The microscopic images as seen above describe the effect of three samples on the HEK 293 cells after 24 hrs of treatment. As seen from figure 26 (a) the number of viable cells was more in control in presence of only growth media, whereas the number of viable cells were less when the cells were being treated with LDH nanopowders as is seen in figure 26 (b). The number of viable cells abnormally decreased when treated with the bare salicylate drug as

seen in figure 26 (c) , thus revealing its cytotoxic nature. When intercalated into the interlayer space of the LDH nanopowders, the cytotoxicity of the SA was decreased as seen from figure 25 (d).

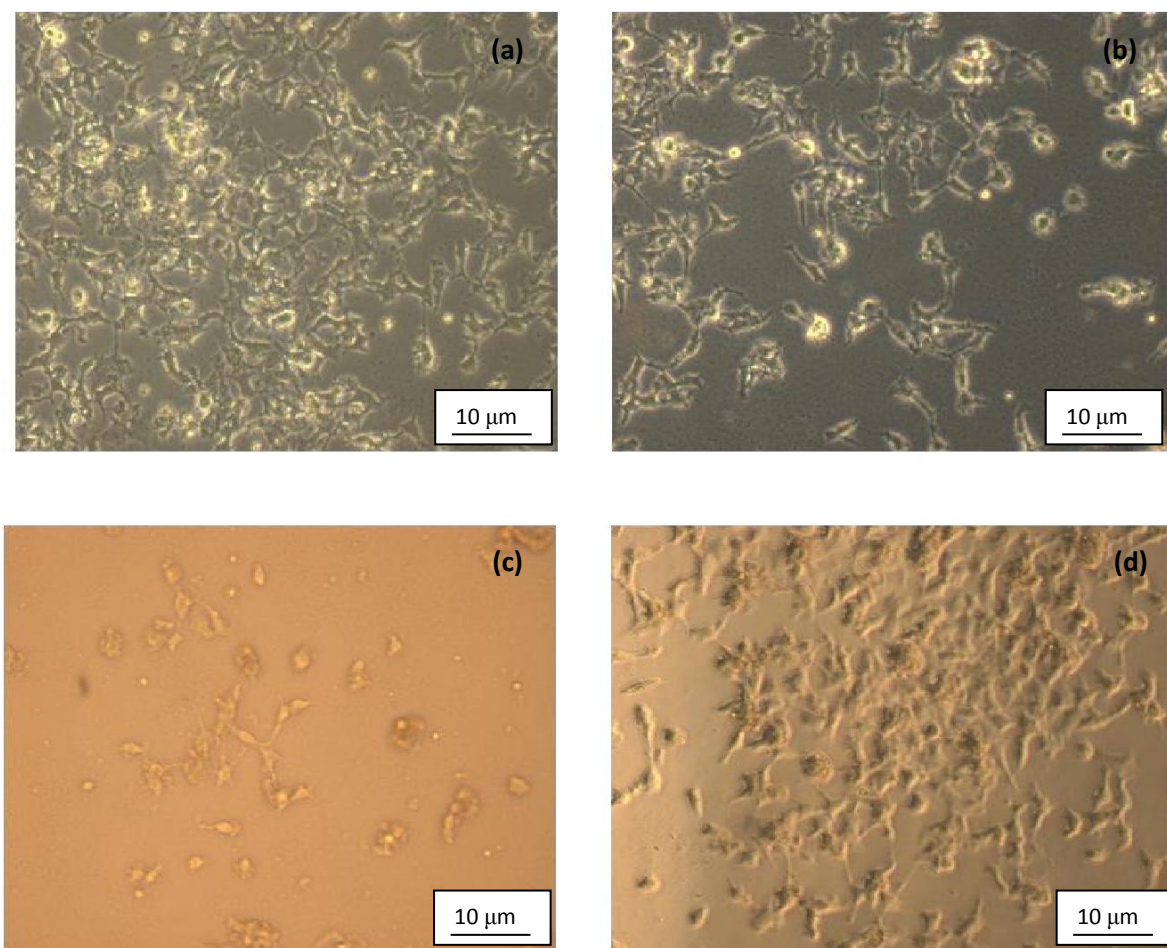


FIGURE 27: Effect of (a) Media (control) (b) LDH (c) SA (d) LDH-SA on the HEK 293 cells after 48hrs of treatment

The microscopic images as seen above in figure 27 describe the effect of three samples on HEK 293 cells after 48 hrs of treatment. As seen from figure 27 (a) the number of viable cells was more in control in presence of only growth media, whereas the number of viable cells was less when the cells were treated with LDH nanopowders as seen in figure 27 (b). The number of viable cells was least when the cell line was treated with bare salicylate drug as seen in figure 27 (c). In comparison, the cell line when treated with the LDH-SA nanohybrid



appeared to be more healthy and higher in number as compared to the bare LDH and the bare SA treated cell lines.

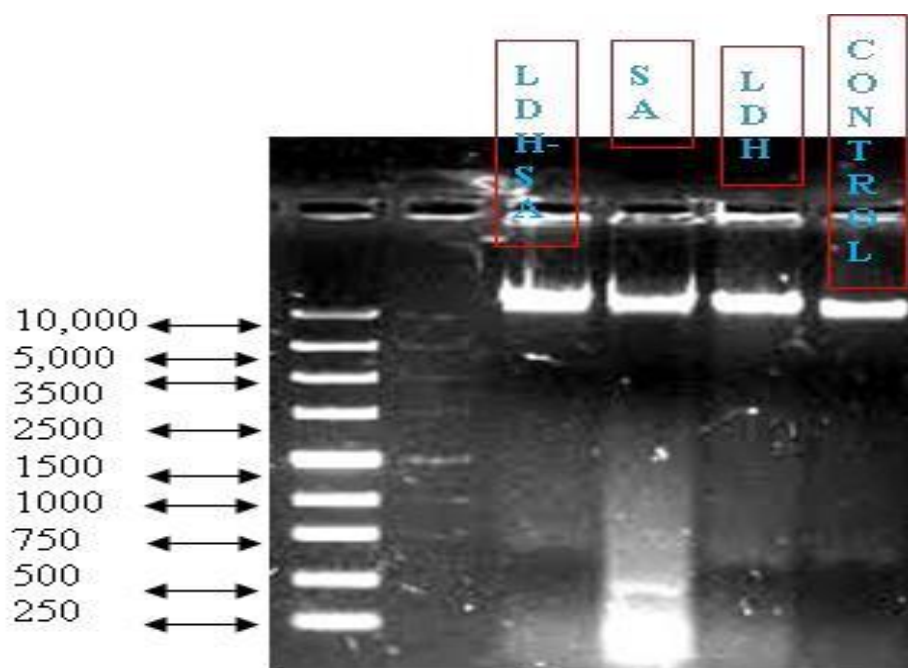


FIGURE 28 : Agarose gel electrophoresis of DNA fragmentation on HEK 293 cells

(a) Lane 1: Control (b) Lane 2: LDH (c) Lane 3: SA (d) Lane 4: LDH-SA.

DNA fragmentation is a key feature to measure cell death. Figure 28 clearly shows the nature of cell growth and their subsequent death due to the treatment of the cells with the test samples after 48 hrs. Excessive cell death was observed in the cell plate treated with that of free Salicylate. The higher amount of cell death, when treated with SA, was also attributed to the higher smear and clear ladder formation observed in the agarose gel electrophoresis as shown in figure 28. When the cells are treated with the intercalated nanohybrid LDH-SA there was very little or in fact negligible amount of cell death, or negligible ladder formation similar to that as observed in the log phase i.e. the control cell plate with no smear being observed in the agarose gel electrophoresis. This proves the higher biocompatibility of the LDH-SA nanohybrid in comparison to the free salicylate.

### 5.13 **REFERENCES:**

1. G.W. Brindley and S. Kikkawa, *Amer. Min.*, 64,836(1979).
2. H.F.W. Taylor, *Miner. Mug*,37,338(1969).
3. B.J Berne, R Pecora, *Dynamic Light Scattering*. Courier Dover Publications (2000)ISBN 0-486-41155-9.
4. H .Zhang, S. H Guo, K. Zou, X.Duan, *Mater. Res. Bull.*, 44, 1062–1069, (2009).
5. M.J.H. Hemandez-Moreno, M.A. Ulibarri, J.L. Rendon and C.J. Sema, *Phys. Chem. Minerals*, 12,34(1985).
6. Z .P Xu, G .Q Lu, *Pure Appl. Chem.* 78 ,1771–1779, (2006).
7. D.L. Bish and G.W. Brindley, *Amer. Min.*, 62,458(1977).
8. S. Miyata, *Clays and Clay Minerals*, 23,369(1975).
9. S. Miyata and A. Okada, *Clays and Clay Minerals*, 25,14(1977).
10. C.J. Sema, J.L. White and S.L. Hem, *Clays and Clay Minerals*, 25,384(1977).
11. PA Mackowiak. A brief history of antipyretic therapy. *Clin Infect Dis.*;31(Suppl 5): S154–156(2000).
12. MZ Hussein, WL Chan. Synthesis of organo mineral nanohybrid material: indole 2carboxylate in the lamella of ZnAl layered double hydroxide. *Mater Chem Phys.*;85 427–431(2004).
13. L. J. Bellamy, *The Infrared Spectra of Complex Molecules*, Chapman& Hall London, pp.433-441, (1975).
14. L. Zhang, Y. Lin, Z.Tuo, D .G. Evans, D. Li, *Journal of Solid State Chemistry* 180 (4) 1230-1235, (2007).
15. G.J. Ross and H. Kodama, *Amer. Min.*, 52,1037(1967).
16. S. Miyata, *Clays and Clay Minerals*, 23,369(1975).
17. S. Miyata, *Clays ad Clay Minerals*, 28,50(1980).
18. O. Marino and G. Mascolo. in D. Dollimore (Editor), *Proc. 2nd Europ. Symp. Thermal Analysis*, Heyden, London,391,(1981).
19. R..S Soumya, S. Ghosh, E .T Abraham, *Int. J. Biol. Macromol.* 46,267–269,(2010).
20. [2] F .S Li, L. Jin, J. B Han, M.Wei, C.J. Li, *Ind. Eng. Chem. Res.* 48, 5590–5597, (2009).

21. [3] B .S Dave, A .F Amin, M .M. Patel, AAPS Pharm. Sci. Tech., 5(2), 77-82, (2004).
22. [4] S.Dash, P. N Murthy, L. Nath and P. Chowdhury ,Acta Poloniae Pharmaceutica n Drug Res, 67(3),217-223,(2010).



## CHAPTER 6: -

### **CONCLUSION & SCOPE OF** **FUTURE WORK**

## 6.1 **CONCLUSION:**

In the present study, Mg Al LDH-salicylate inorganic –organic nanohybrid was synthesized, and its effectiveness in the controlled and sustained release of salicylate was evaluated in vitro. It has also been shown that SA in the intercalated form inside the interlayer space of Mg-Al LDH was less cytotoxic to human embryonic kidney cell line as compared to the sole salicylate drug taken orally or intravenously. The results of the aforementioned work can be summarized as follows.

- (i) LDH was synthesized in the particle size range of 40 -70 nm.
- (ii) Successful intercalation of Salicylate in the interlayer space of Mg-Al-LDH was confirmed by XRD data and FTIR Spectroscopy of the intercalated nanohybrid. Salicylate is loaded to the extent of 24 wt% in the LDH salicylate formulation.
- (iii) It was evident that the SA drug release from LDH followed first order release kinetics with a satisfactory coefficient of 0.9816. The drug release rate followed an exponential dependence with respect to incubation time with a combination of drug diffusion and LDH dissolution mechanism.
- (iv) Cytotoxicity of the samples were determined using MTT Assay and the Hemolysis tests that showed that SA intercalated into the interlayer of LDH was less cytotoxic as compared to bare SA drug.
- (v) Further DNA fragmentation by the gel electrophoresis method showed that LDH-SA treated cells underwent less cell death as compared to the bare SA treated kidney cells, which supports higher biocompatibility of LDH-SA nanohybrid to kidney cell than the bare SA drug.
- (vi) The advantage of using SA intercalated LDH nanocarrier instead of bare NSAID on minimizing damage to human kidney cells is evidently supported by all the cytotoxicity tests.

- (vii) This work supports that Mg AL-LDH nanopowder can be a very effective carrier for controlled and sustained release of NSAIDs under physiological conditions.

## 6.2 **SCOPE OF FUTURE WORK:**

In recent years, inorganic materials have inspired considerable interest in the fields of chemical, biological, and drug delivery applications. A new type of layered inorganic material, layered double hydroxides (LDHs), has especially generated a lot of interest for research. For example, LDHs showed potential applications for CO<sub>2</sub> capture materials, biomolecular reservoirs, catalysts, contrast agents, and for agricultural applications. For pharmaceutical applications, LDHs have given rise to great interest because the nanocarriers can control the release of active drugs and biological molecules for the design of targeting delivery systems.

The feasibility of LDH nanoparticles to develop organ specific targeting by incorporation of an NIR fluorescent dye, indocyanine green(ICG), in the layered structures of amine-modified LDHs can be studied. The produced LDHs–NH<sub>2</sub>–ICG complexes were further coated with different amounts of chitosan molecules by a covalent cross-link of amino groups between the LDHs–NH<sub>2</sub> and chitosan molecules through glutaraldehyde as a cross-linking agent. The combination of LDHs and ICG can apply to invivo optical imaging because the excitation and emission at long wavelengths(ex: 780 nm; em: 820 nm) in the NIR window where blood and tissue are relatively transparent. We can easily control the bio-distribution of LDHs by using different amounts of a biodegradable polymer such as chitosan coated on the external surfaces of LDHs–NH<sub>2</sub>–ICG. It can be exhibited that the chitosan-coated LDHs–NH<sub>2</sub>–ICG complexes possess high biocompatibility, high fluorescence intensity, highly organ-specific targeting and low cytotoxicity. The chitosan-coated LDH surfaces can increase the stability of the nanocomposites; furthermore, the targeting molecules can be conjugated in the external surfaces of the chitosan molecules through a further reaction with the amino groups.

## CURRICULUM VITAE

### **SOUMINI MONDAL**

D/O, Rabindra Nath Mondal

VIJAYA TOEWR, FLAT NO-E1,Block-  
B SUBHASPALLY MAIN ROAD,  
BURNPUR-713325,BURDWAN ,  
WEST BENGAL.

MOB NO.-9475676071

Email.- [soumini15@gmail.com](mailto:soumini15@gmail.com)

Date of Birth- 25-07-1988

EDUCATION :- B.Tech (Bio-Technology), 2012, The Neotia Institute of  
Technology Management and Science , (WBUT).

Research Interest : Bioceramics, Biomaterials, Drug-Delivery.

### LIST OF PUBLICATIONS:-

- “Sodium Salicylate Intercalated Mg AL- Layered Double Hydroxide”, Soumini Mondal, Sudip Dasgupta, National Institute of Technology Rourkela, Ceramic Engineering, Rourkela, INDIA (Communicated).

### CONFERENCES :

International conference of Indian Ceramic Society, presented paper title “Sodium Salicylate Intercalated Mg AL- Layered Double Hydroxide”, at Jamshedpur Feb 2015.

